POLITECNICO DI MILANO

School of Industrial and Information Engineering

Master Degree in Materials Engineering and Nanotechnology

Chemistry, Material and Chemical Engineering Department "Giulio Natta"

MECHANICAL AND CALORIMETRIC CHARACTERIZATION OF NOVEL ENVIRONMENTALLY FRIENDLY COPOLYMERS

Supervisor: Prof. Francesco Briatico Vangosa

Master Degree Thesis:
Carla Franculli
N° 787471

Academic Year 2012/2013

Table of contents

Figures

Tables

Abstract

This work presents the results obtained from the calorimetric and mechanical characterization of new novel random copolyesters, constituted by butylene adipate (BA) and butylene 1,4-cyclohexanedicarboxilate (BCHD) monomers, available in two different molar ratio and of the two respective homopolymers. Besides of the composition effect, due to the availability of batches with different molecular weight, it was also studied the effect of this variable on the mechanical behaviour.

The calorimetric analysis has highlighted the effect of the composition on characteristic temperatures and crystallinity of the materials and, considering literature data, has allowed to conclude that the crystalline phase of the copolymers is essentially constituted by only the BCHD monomer while the BA constitutes the amorphous phase.

From uniaxial tensile tests it was possible to obtain a significant effect of the molecular weight on the PBA and copolymers yielding mechanisms, whereby only above a similar threshold value for all the materials plastic flow and following strain hardening were observed after yielding. This phenomena, together with the dependence of Young's Modulus, stress and strain yielding – for materials with similar molecular weight- from polymer composition seems to be in agreement with the model suggested by the calorimetric results.

On the other hand, toughness was determined through the essential work of fracture method. Because of the limited availability of material, fracture tests were performed only on one copolymer and on the commercial copolymer (Ecoflex). As a result it was noticed that the new material has a higher toughness than Ecoflex and comparable with the literature reported value for PE.

The field of applications of these materials is food and agricultural packaging, which traditionally employs PE and another innovative films (Ecoflex). The aim of the use of PBA-co-PBCHD copolymer is the substitution of those traditional materials in order to achieved a higher biodegradability rate, maintaining the same performance.

The results show the high potential of these studied novel copolymers as a future replacement of materials already in use.

Sommario

In questo studio sono presentati i risultati della caratterizzazione calorimetrica e meccanica di nuovi copoliesteri random, costituiti da butilene adipato (BA) e da butilene 1,4-cicloesanodicarbossilato (BCHD), disponibili con due diverse frazioni molari, e dei due omopolimeri corrispondenti. Oltre all'effetto della composizione, data la disponibilità di lotti a diverso peso molecolare, si è considerato anche l'effetto di tale variabile sul comportamento meccanico.

L'analisi calorimetrica ha evidenziato l'effetto della composizione sulle temperature caratteristiche e sulla cristallinità dei materiali e, insieme a dati di letteratura, ha permesso di ipotizzare che nei copolimeri la fase cristallina sia costituita essenzialmente da segmenti di BCHD, mentre il BA vada a costituire essenzialmente la fase amorfa.

Da prove di trazione uniassiale si è potuto riscontrare un effetto significativo del peso molecolare sui meccanismi di snervamento del PBA e dei copolimeri, per cui solo al di sopra di un valore di soglia, simile per tutti i materiali, si osserva, dopo lo snervamento, un flusso plastico e un successivo "*strain hardening*". Tale fenomeno, insieme alla dipendenza di modulo e di sforzo e deformazione di snervamento – per materiali di pari peso molecolare – dalla composizione del polimero, sembra essere in accordo con il modello suggerito dai dati calorimetrici.

La tenacità è stata invece determinata impiegando il metodo del lavoro essenziale di frattura. Le prove, effettuate per mancanze di materiale solo su un copolimero e su un copoliestere commerciale (Ecoflex), hanno dimostrato che il nuovo materiale ha una tenacità più elevata e confrontabile con quella di PE riportata in letteratura.

Il campo di applicazione di questi materiali è quello del packaging, con sbocco nei campi alimentare ed agricolo, al fine di sostituire materiali tradizionali, come il PE, o innovativi, come l'Ecoflex, garantendo un tasso di biodegradabilità maggiore a parità di altre prestazioni rispetto ai materiali già in uso.

I risultati di questo lavoro dimostrano la potenzialità dei materiali studiati come sostituti dei materiali attualmente in uso in campo alimentare e agricolo.

Introduction

Nowadays polymers are widely employed in a great variety of applications, thanks to their low cost and, at the same time, excellent mechanical and thermal properties. Dwelling on the packaging field, the most used polymers are poly(ethylene) PE, poly(ethylene terephthalate) PET and poly(butylene terephthalate) PBT. These conventional thermoplastic polymers, as said before, show excellent thermal and mechanical properties, low permeability, chemical resistance and low cost; nevertheless they are mainly petroleum-based materials, thus deriving from non-renewable sources. In addition they are also characterized by high resistance to atmospheric and biological agents. In order to solve plastic waste environmental impact problems, academic and industrial research is showing an increasing interest in the development and study of novel environmental-friendly polymers, which can be an efficient alternative to the conventional thermoplastic polymers.

By considering these novel "green" polymers, it's worth recalling two approaches, the biopolymers and the novel copolymers. Among the former, PLA poly(lactic acid) and PHB poly(R)-3-hydorxybutyrate are to be mentioned, as these biopolymers present impressive advantages: on one side, they are produced from alternative resources and with low energy consumption and are biodegradable or characterized by the possibility of easy recover of monomers; on the other side, nevertheless, these biopolymers generally combine these excellent features, with poor physical properties and sometimes high costs. For what concerns the novel copolyesters, instead, not only are they characterized by good mechanical and physical properties, they also show a high biodegradability and biocompatibility. One of these copolyesters is a poly[(butylene adipate)-co-(butylene terephthalate)], produced by BASF and on the market under the Ecoflex trade name (Figure 1.1).
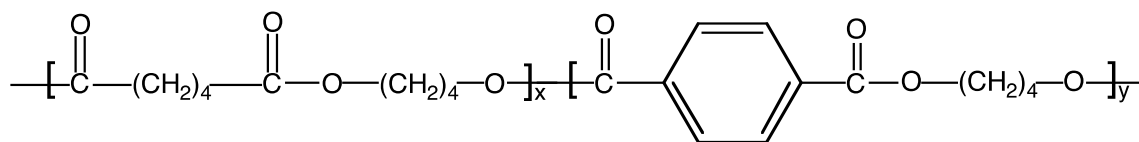
Figure 1.1 Ecoflex molecular structure

Ecoflex is completely biodegradable and can be used in applications such as mulch films for agriculture, cling-warp films or coatings for packaging and breathable films (1) (2). The presence of an aromatic ring gives high melting temperatures, about 120°C, and improves the mechanical and physical properties. However, the aromatic ring partly limits the biodegradation rate of Ecoflex. To overcome this limit, recently a new fully aliphatic copolymer has been proposed, PBA-co-PBCHD, poly[(butylene adipate)-co-(butylene 1,4-cyclohexanedicarboxylate)] (Figure 1.2).
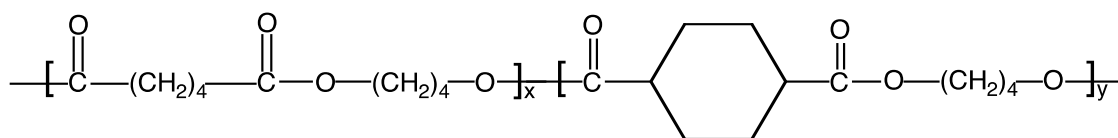
Figure 1.2 PBA-co-PBCHD molecular structure

The presence of an aliphatic ring enables the material to have good thermal and mechanical properties and to maintain or improve the biodegradation rate with respect to the Ecoflex case; furthermore there is the possibility that it might be produced by renewable sources. The peculiarity of this novel copolymer is the opportunity to easily modulate the physical properties slightly changing the chemical structure, for example by varying the cis/trans ratio of the 1,4 cyclohexylene ring in BCHD units.

Even if this new copolymer class have been deeply investigated from a chemical and structural point of view (3) (4) (5) (6) (7) (8) (9) (10) (11) (12), few works have been carried out on their mechanical characterization and their possible industrial application. The field in which these novel copolymers might find applications is the Ecoflex one. Thence in this work the calorimetric and mechanical properties of the copolyester PBA-co-PBCHD100 will be investigated, giving special attention to the effect of the structural composition, the different percentage of PBA and PBCHD or to the influence of the molecular weight or of the chemical kinetics. Finally, in view of using these new materials in flexible packaging or mulch films for agriculture, the tensile response and toughness of copolyesters will be investigated and compared with those of PE and Ecoflex.

11

1.1. State of the art

The previously mentioned novel-environmental friendly polymers were synthesized and already analysed, from a chemical, thermal and compositional point of view, by the research group of Prof. Annamaria Celli at the University of Bologna. Starting from the characterization of the homopolymer PBCHD (Figure 1.3), these studies emphasize the importance of the 1,4-cyclohexylene units in determining the final thermal and mechanical properties (3).
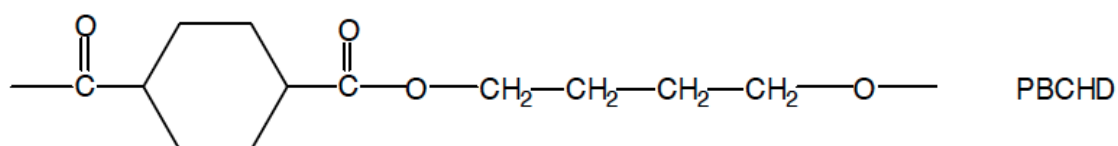
Figure 1.3 Poly(butylene 1,4-cyclohexanedicarboxylate) molecular structure

Indeed, it is known that the C_6 ring can exist in two isomeric forms, cis and trans (Figure 1.4).

trans   *cis*
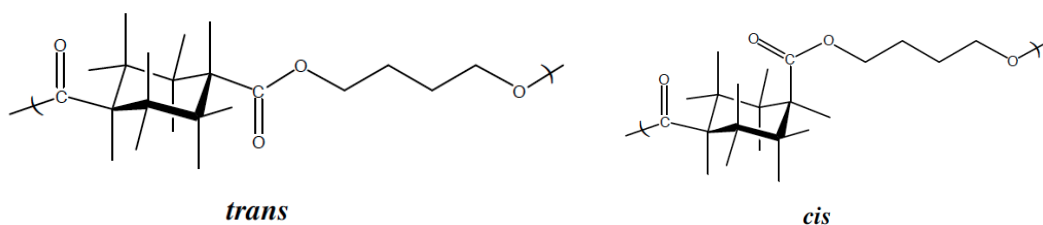
Figure 1.4 Trans and cis isomeric forms of BCHD

By varying the cis/trans ratio of the cycloaliphatic units it is possible to vary the final properties of the material very significantly. In particular the $PBCHD_{xx}$ is synthesized starting from the Dimethyl 1,4-cyclohexanedicarboxylate (DMCD) and 1,4-Butanediol (BD) (Figure 1.5), where xx indicates the percentage of C_6 rings derived from DMCD in trans configuration.

Dimethyl 1,4-cyclohexanedicarboxylate (DMCD)

1,4-Butanediol (BD)   HO-(CH$_2$)$_4$-OH

Figure 1.5 DMCD and BD molecular structures

The cis/trans ratio is determined by H NMR on the final polymer, in order to determine its influence on the thermal stability, the thermal transition temperature and the mechanical behaviour. From a thermogravimetric analysis, observing the maximum degradation rate temperature T_D, it appeared that all the samples have a really similar behaviour, thence the cis/trans ratio influence on the thermal stability was excluded (3) (6). However, by a comparison between the PBT T_D (408°C) and the PBCHD$_{100}$ one, the latter is 13°C higher, indicating that the substitution of the aromatic ring with an aliphatic unit improves the thermal stability of the materials (Figure 1.6).
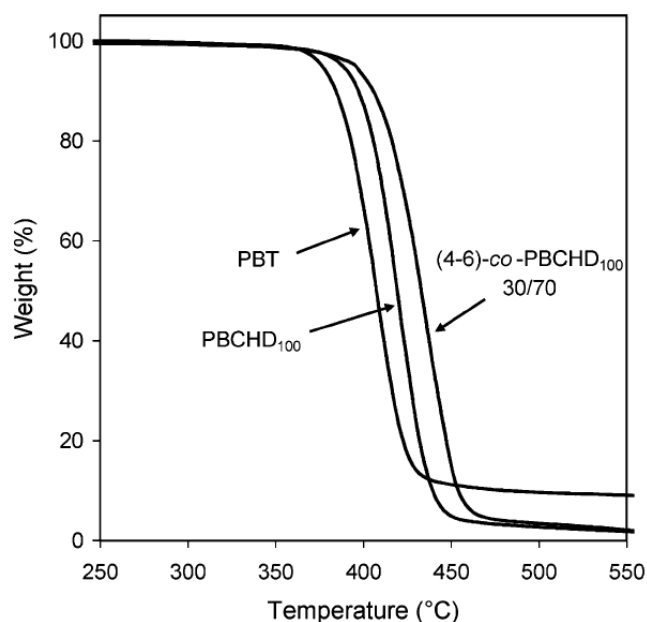
Figure 1.6 Thermogravimetric curves, obtained in nitrogen at 10°C/min, of PBCHD100, PBA(4-6)-co-PBCHD100 30/70, and a commercial samole of PBT

From the DSC analysis, instead, the literature (3) (6) reports that only the samples with a trans content $\geq$ 72% crystallize and the exothermal peaks become more and more intense and narrow as the trans content increases (Figure 1.8).
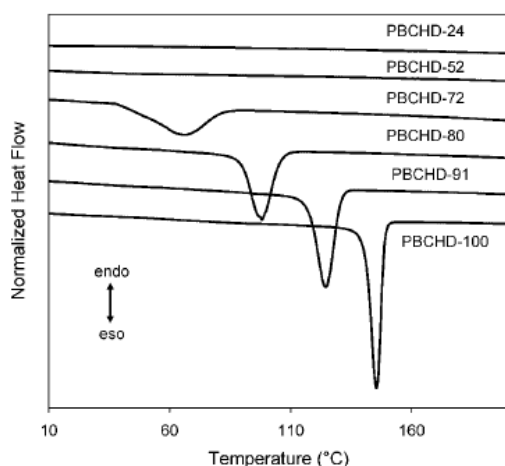
Figure 1.7 DSC thermograms obtained during the cooling from the melt at 20 K/min
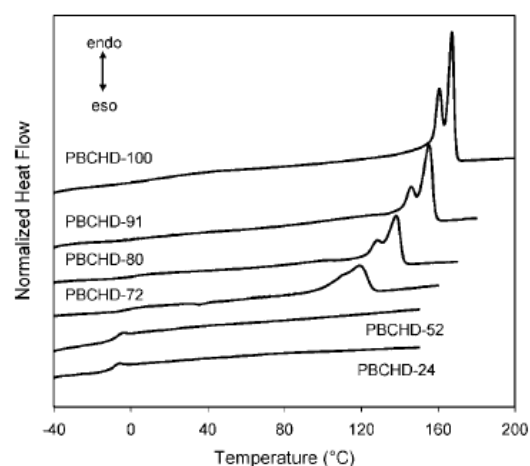
Figure 1.8 DSC thermograms obtained during the heating scan at 20 K/min

In particular, for $PBCHD_{72}$ to $PBCHD_{100}$ T_C increases by about 80K and the enthalpy doubles, this indicating that the trans configuration improves the capacity of the samples to crystallize. Thence PBCHD with a trans content higher than 72% is crystalline and the melting temperatures increase considerably with the increment of the trans content, from 119°C for the 72%trans to 167°C for the 100% trans. On the other hand, it is shown that the $PBCHD_{52}$ and $PBCHD_{24}$, with the lowest percentage of trans stereoisomer, are not able to rearrange towards an ordered state at all and the second heating scan, given form literature (6), confirms that they are completely amorphous materials. The tendency of the aliphatic rings in trans configuration to favour the crystalline phase can be explained by considering that in this configuration the polymeric chain assumes a "stretched" form and a high symmetry, which favours the chain packing (6). Cis isomer, instead, introduces kinks into the chain, hindering the formation of stable crystals. As for the melting temperature, the glass transition temperature increases with the increment of the trans percentage, for example from $PBCHD_{24}$ to $PBCHD_{100}$ the T_g increases by 28 degrees, from -10°C to 18°C. To explain the effect of the stereochemistry in the cycloaliphatic ring on the glass transition, it is necessary to recall that the most important factors influencing the T_g values are chain flexibility, symmetry and steric hindrance and bulkiness of the side groups attached to the backbone chain. In 1,4 ring polymers a better molecular fit is achieved in the polymer backbone, resulting in a better chain packing and improved orientation, which would restrict the movement of the chains upon heating. The same consideration can be made for PBCHD, where the trans isomer is more symmetrical than cis. Moreover, increasing trans % the T_g increases also for the notable level of crystallinity, which creates numerous impediments to the chain mobility in the amorphous state. This said about the PBCHD, the

same kind of studies was also conducted on the PBA and on the copolymers PBA-PBCHD (Figure 1.9).
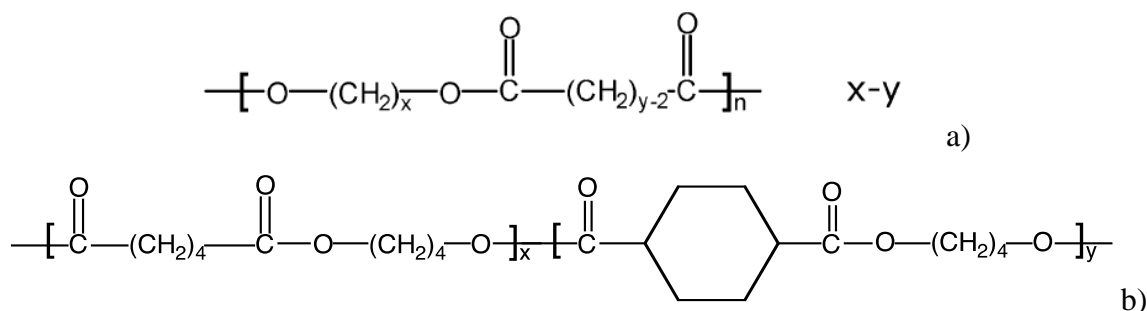
Figure 1.9 A)PBA molecular structure B) PBA-co-PBCHD molecular structure

First of all it is important to underline that the poly(alkylane dicarboxylate) exists in different structure, depending on the length of the –(CH_2)- sequences and, from DSC on different samples, it is evident that melting temperatures and enthalpies increase with the length of the aliphatic chain (4); in this thesis, however, only copolymers derived from 4-6 will be investigated. It is also worth remembering that the PBA is a biodegradable polymer. As said before the PBCHD has a remarkable resistance to the thermal degradation, instead, from thermogravimetric analysis, it appears that the PBA begins to lose weight at about 300°C and shows a degradation curve shifted at lower temperatures (4). Nevertheless, the copolymers are characterized by a slightly higher thermal stability (Figure 1.6), also respect to the PBCHD homopolymer (6).

The literature DSC analysis shows, also for the PBA, very narrow and intense exothermic peaks on cooling. The copolymers show the ability to crystallize too, although the crystallization temperature and the crystallization enthalpy tend to be reduced with the decrement of the PBCHD unit content (Figure 1.10).
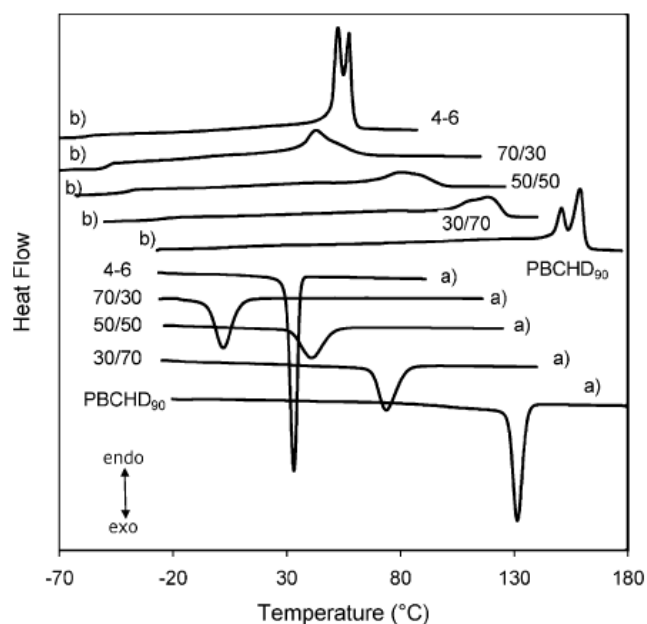
Figure 1.10 DSC traces obtained at 10°C/min during the cooling from the melt (curves a) and during the seconf heating (curves b) for the series of PBA(4-6)-co-PBCHD₉₀ samples.

Furthermore, the DSC curves, shown by literature, present complex melting peaks, discussed as a melting-recrystallization-remelting processes. The copolymers peaks are different from the homopolymer ones, they are broader and with lower intensity. This might mean that the size distribution of the crystals is more scattered. In order to better understand the crystallization and melting behaviour of the copolymers, in literature (6) a wide-angle x-ray diffraction (WAXD) analysis is shown. The WAXD spectra (Figure 1.11), obtained from a test at room temperature on samples previously molten and cooled from the melt at 10°C/min, shows for the PBA the crystalline α-form typical profile, which is the thermodynamically most stable phase for the polymer (6); for the PBCHD, instead, it's possible to observe four main peaks. Also the copolymers are characterized by the presence of relatively intense diffraction peaks, which confirm the presence of a crystalline phase for all the PBA-co-PBCHD copolymers.
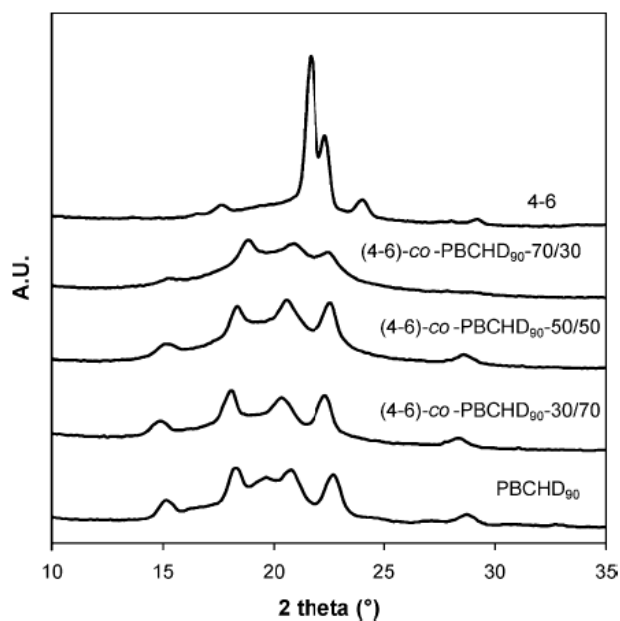
Figure 1.11 X-ray diffraction patterns of PBA(4-6)-co-PBCHD$_{90}$ samples

From an analysis of the diffraction patterns, it seems that all the copolymers are characterized by the presence of the BCHD crystalline phase, also at very low content of BCHD, for example for the 70/30. Thence the PBCHD crystalline phase should not be hindered by the PBA, even for a content of 30% of PBCHD. Moreover, the crystallization enthalpies, normalized with respect to the PBCHD content, are in agreement with the crystallization enthalpy obtained by experiments on the 30/70 and 50/50 (6), and also this result supports the theory according which only the PBCHD crystallizes. In any case the crystallization of PBA is hindered, may be due to the low crystallization rate of PBA (4-6), characterized by short aliphatic sequences. During the cooling from the melt, the competition between the crystallization rates of PBCHD and PBA crystals favours the growth of the PBCHD crystalline phase. The PBCHD crystals dominate in the whole range of compositions and the PBA tend to remain in the amorphous state. However considering copolyesters with the BCHD$_{50}$, the BCHD cannot crystallize due to its too low trans content. As said before the PBCHD with trans content <72% is a fully amorphous material, therefore in the copolymers PBA-co-PBCHD$_{50}$ only PBA (4-6) units is able to crystallize, as shown in figure 1.11. The copolymers, investigated in this work, are made by the PBCHD$_{100}$, in this case the high percentage of trans isomer makes the crystallization of PBA (4-6) units extremely difficult (6). The T$_{g}$ values tend to increase with the increment of the BCHD units, according to the fact that the cycloaliphatic ring has a more rigid structure than the -(CH$_2$)- sequences, and even if the PBA, which is preferentially in the amorphous state, induces a decrement of T$_{g}$, as final result the glass transition temperature does not change very significantly. So the effect of the copolymer composition in the thermal behaviour of semi-

crystalline random copolymers can be described in terms of two-phase systems, where a crystalline phase, BCHD units, coexists with an amorphous one, BA units.

1.2. Essential work of fracture

Materials for packaging are usually in the form of thin films, thence it follows that it's important to characterize the mechanical behaviour with the appropriate method. Focusing on protective packaging for the food industry a very important issue, with respect to safety, is films integrity, as a failure of the packaging would imply a probable contamination of the content. Thus fracture behaviour has to be assessed and doing this it must be reminded that the toughness of materials depends on the stress state, which in its turn is controlled by the sample thickness (Figure 1.12). The conditions, in which the material can be found, vary from plane stress state to plane strain state as function of the thickness (Figure 1.12).
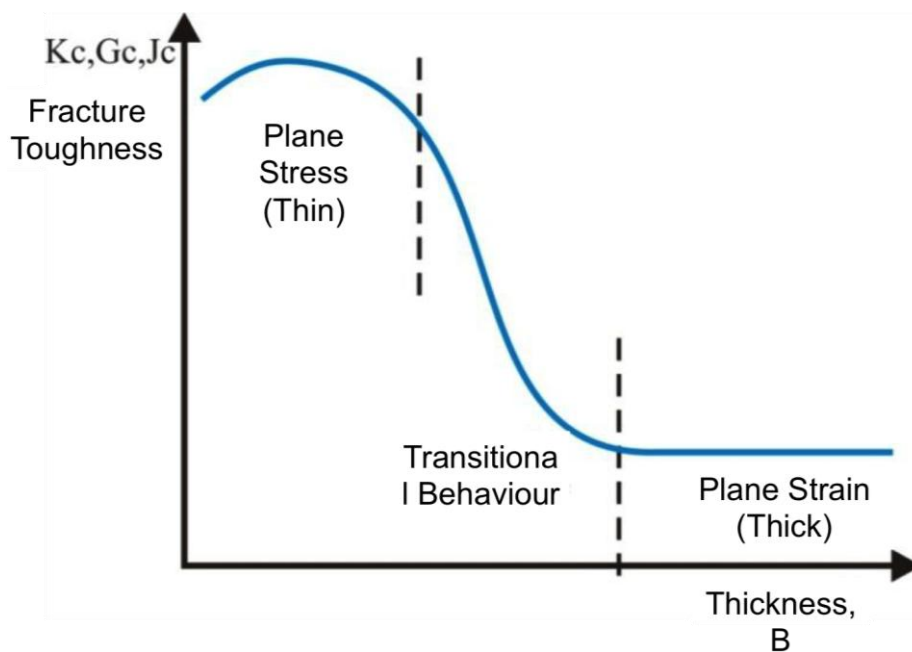
Figure 1.12 Thoughness dependence on thickness (13)

Thin films work in plane stress condition and, in this case, a proper method to characterize the fracture behaviour is the Essential Work of Fracture (EWF) method, which allows the measurement of the energy per unit area, necessary to create the fracture surfaces and referred to as "EWF". The foundations for the development of the EWF were laid by Broberg (14), who suggested separating the region around the crack tip into two portions: one (process zone) is where the fracture phenomenon occurs as creation of new surfaces, the other (plastic zone) is where plasticization occurs. The idea, developed by Cotterell, Reddel and Mai for metals (15)

(16) and then extended to ductile polymer films (17) (18), was that the global fracture energy W_f is given by two contributions, referred to the two different regions around the crack tip:

$$W_f = W_e + W_p \qquad (1.1)$$

W_e is the essential work required to create new surfaces in the process zone, W_p, instead, is the non essential work required for the permanent strain that occurs in the plastic zone.

The essential work can be investigated performing fracture tests on Double Edge Notched samples tested in tension (DENT) Figure 1.13 (19).
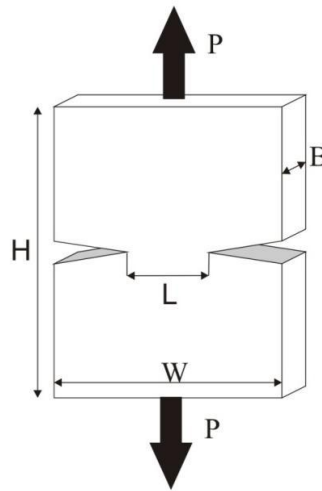
Figure 1.13 DENT geometry sample (19)

In Figure 1.13 B is the thickness, W the width and H the height of the specimen, while L indicates the length of the cross section, which is called "ligament".

As suggested in equation 1.1 the energy W_f is spent in two different processes, the essential work for the crack propagation w_e, which is acting on the area of the notched process zone, $w_e BL$, and the plastic work, $w_p \beta BL^2$, in which w_p is the energy density dissipated in the area βBL^2, indicated by the shape factor β. Thus

$$W_f = w_e \mathrm{BL} + w_p \beta \mathrm{B} L^2 \qquad (1.2)$$

Referring the total work, W_f, to the area of cross section along which the crack propagation occurs, the total specific energy of fracture is obtained:

$$w_f = w_e + w_p \beta \mathrm{L} \qquad (1.3)$$

From this relation it is possible to observe a linear correlation between the work of fracture and the ligament length. Furthermore, when the ligament length is zero (L=0), the work of fracture corresponds exactly to the essential work ($w_p = w_e$), while the slope of the curve is referred to the plastic work and corresponds to $w_p \beta$.

From an operational point of view, in order to measure the essential work of fracture, tensile tests at constant rate (10 mm/min) on a set of samples with the same thickness B and length H, but with different ligament length have to be carried out. The crack propagates along the ligament until the failure occurs. From these tests, the total dissipated energy is obtained as the area under the load (P)-displacement (δ) curve:

$$W_f = \int_0^{\delta_{BREAK}} P d\delta \qquad (1.4)$$
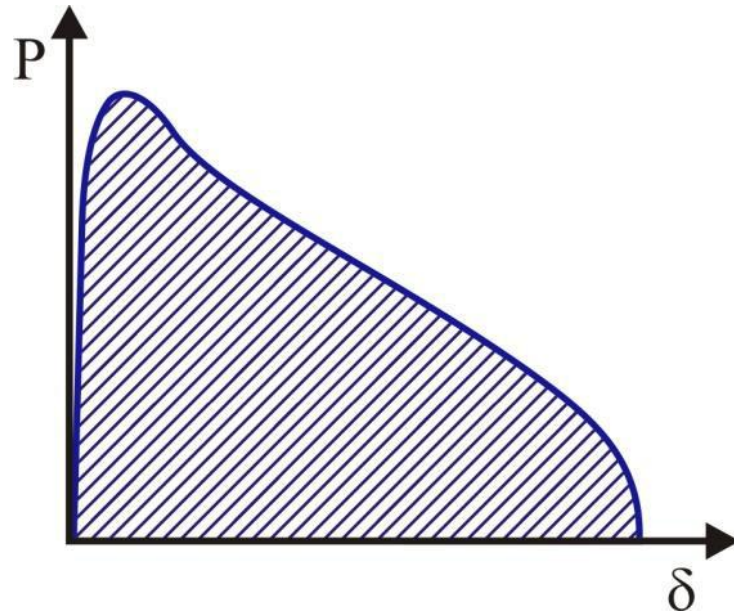
Figure 1.14 Work of Fracture from the Load-Displacement curve

and the specific energy of fracture w_f is:

$$w_f = \frac{W_f}{BL} \qquad (1.5)$$

By reporting the w_f values as a function of the ligament, a linear correlation should be found and, fitting the experimental points, the intersection with the y-axis is exactly the essential work of fracture w_e, while the slope represents the value βL (Figure 1.15).
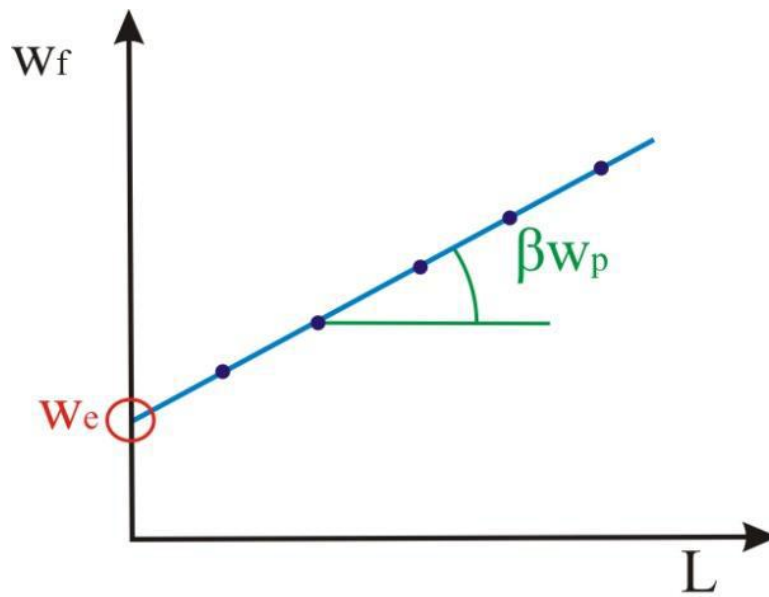
Figure 1.15 Work of Fracture as function of ligament length

In order to apply the EWF method, some requirements should be verified:

- The ligament has to be completely yielded before the onset of the crack;
- The load-displacement curves have to be homothetic (Figure 1.16).

These conditions are necessary in order to satisfy the hypothesis according to which the fracture phenomenology should be independent on the ligament length.
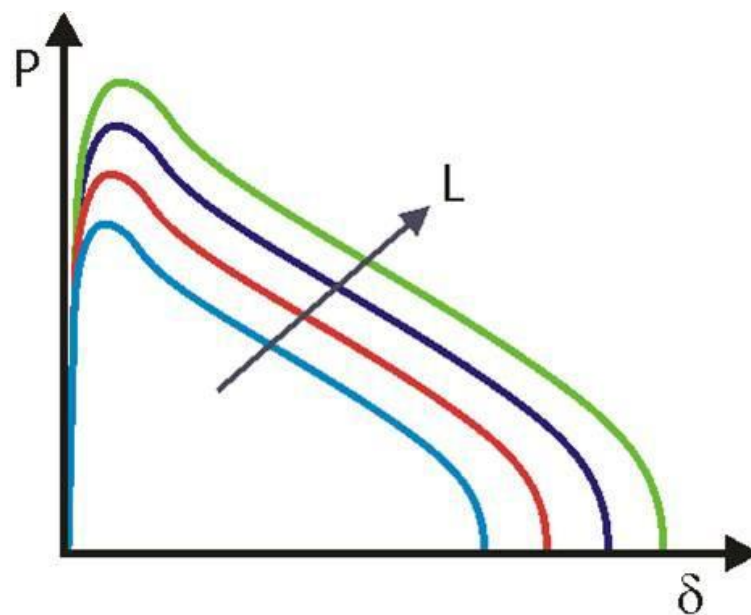
Figure 1.16 Homotetic Load displacement curves

Since in this work the available material was in low quantities, it was not possible to perform a considerable number of tests at different lengths of ligament. To be more precise, the EWF was carried out only on the Ecoflex and on the copolymer PBA-co-PBCHD$_{100}$ 70/30; about the former, experimental points at 5 different lengths of ligament were obtained: two extreme values (5 and 15 mm), one middle point (10 mm) and two points at the same distance from the middle one (8 and 12 mm). For the copolymer PBA-co-PBCHD$_{100}$ 70/30, instead, experimental points only at 3 different lengths of ligament (the two extreme values and the middle point 5, 10, 15 mm) were obtained.

Due to the limited number of tests performed, some doubts arise on the statistical validity of the measures obtained.

In order to measure the confidence interval on the expected w_e value, a statistical method given by Helmut Steininger (BASF) was applied. Through this method it is possible to obtain an interval in which the 95% of probability to find the intersection with the y-axis exists. In this way the precision of the experimental data w_e could be verified.

Materials

The materials considered in this study are two homopolymers, PBA and $PBCHD_{100}$ and two copolymers with different compositions, PBA-*co*-$PBCHD_{100}$ 50/50, containing 50% of both the monomers, and PBA-*co*-$PBCHD_{100}$ 70/30, containing the two monomers in a 70/30 ratio, synthesized and supplied by the research group of the University of Bologna. Moreover, also the Ecoflex was studied.

2.1. Synthesis of the materials

2.1.1.   PBA poly(butylene adipate)

PBA is synthesized through polycondensation of dimethyl adipate (DMA) and 1,4-butanediol (BD) (Figure 2.1).

Dimethyl adipate (DMA) $H_3COOC\text{-}(CH_2)_4\text{-}COOCH_3$

1,4-Butanediol (BD) $HO\text{-}(CH_2)_4\text{-}OH$

$$\left[O-(CH_2)_x-O-\overset{\overset{O}{\|}}{C}-(CH_2)_{y\text{-}2}\text{-}\overset{\overset{O}{\|}}{C} \right]_n \quad x\text{-}y$$
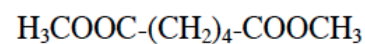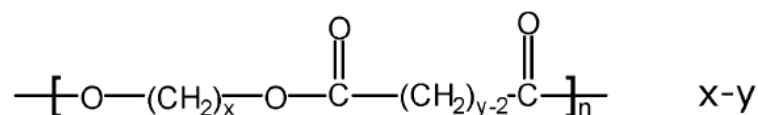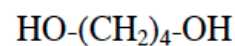
Figure 2.1DMA, BD, and PBA molecular structures

In this work the PBA, which will be investigated, is the 4-6, where 4 and 6 are respectively x and y.

2.1.2. PBCHD poly(butylenecyclohexanedicarboxylate)

PBCHD$_{xx}$ is synthesized in a two-stage process, starting from 1,4-cyclohexane dicarboxylate (DMCD) and 1,4-butanediol (BD) (Figure 2.2).
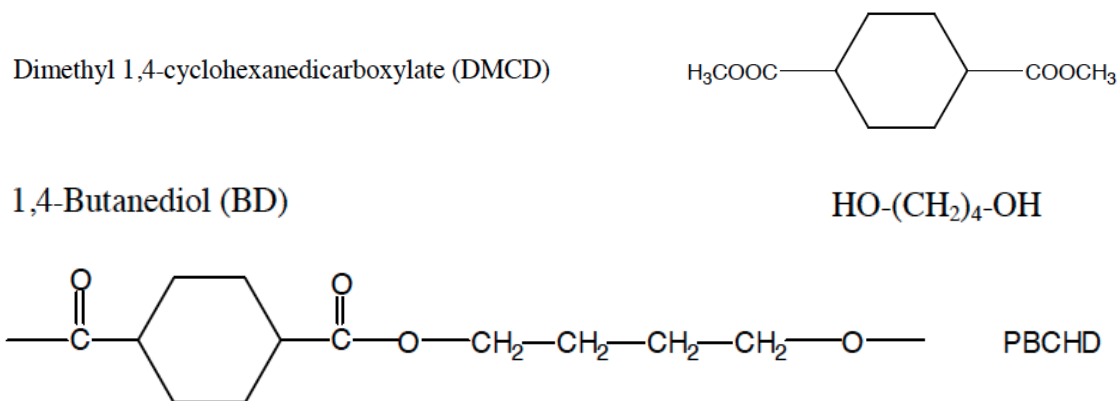
Figure 2.2DMCM, BD and PBCHD molecular structure

The 1,4-cyclohexylene ring can exist in two isomeric forms, *cis* and *trans* (Figure 2.3).
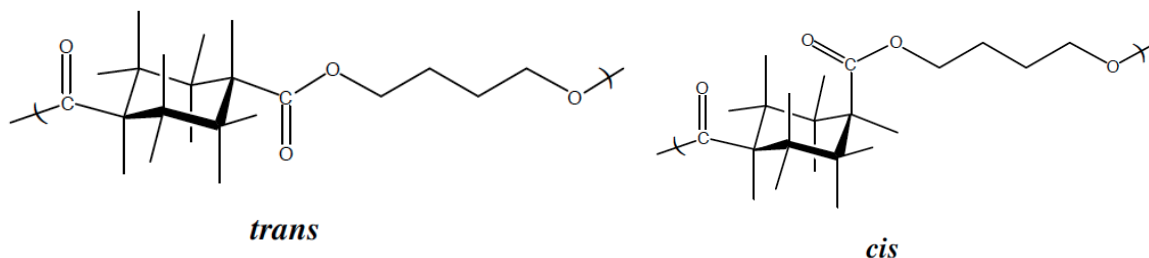
Figure 2.3 trans and cis isomeric forms

The percentage of C$_6$ rings in *trans* configuration is indicated in the name by the letters xx, indeed the homopolymer studied, PBCHD$_{100}$, is completely in the *trans* isomeric form. As said before, by varying the *cis/trans* ratio of the cycloaliphatic units is possible to vary significantly the final properties of the material.

2.1.3. PBA-*co*-PBCHD$_{100}$

The copolymers derived from BD, DMA and DMCD are random and named PBA(4-6)-*co*-PBCHD$_{xx}$-a/b, where a/b is the feed molar ratio of DMA/DMCD. The process that occurs is a polycondensation.
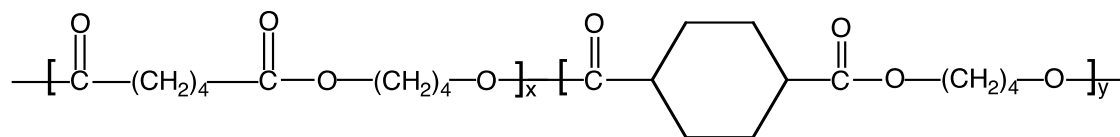
In this work two copolymers will be investigated. In particular the two molar ratios used are 70/30 and 50/50.

2.1.4.   Ecoflex

Ecoflex is a random poly(butylene adipate-co-butylene terephthalate) copolymer, constituted by 54 mol% BA and 46 mol% BT, already on the market and supplied by BASF.
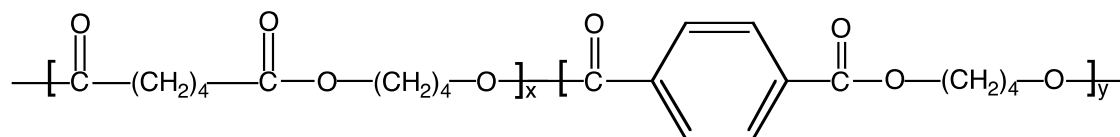
2.2. Molecular Characterization

Each investigated homopolymer and copolymer was available in different molecular weights. Table 2.1 reports all the studied materials, along with their average molecular weight and polydispersity index.

Table 2.1 Studied Materials, their molecular weight and polidispersity index, the data marked as * are from (6) (20)

MATERIAL	LABEL	$M_w \times 10^{-3}$	(4-6)/PBCHD o PBT	% trans PBCHD	M_w/M_n
PBA	PBA_49	49.1			2.1
	PBA_57	56.9			2.2
	PBA_90*	90			2.5
PBA-PBCHD$_{100}$70/30	70/30_58	58			2.6
	70/30_62	62	64/36	100	2.4
	70/30_95*	95.4	64/36	100	2.1
PBA-PBCHD$_{100}$50/50	50/50_40	39.6	47/53	98	2
	50/50_58	58.4	48/52	100	2.3
	50/50_64	63.9		98	2.7
	50/50_74*	73.6	47/53	100	2.3
PBCHD$_{100}$	PBCHD$_{100}$_57	56.6		100	2.2
	PBCHD$_{100}$_73*	73.4		100	2.5
	PBCHD$_{100}$_83	82.6		99	2.5
	PBCHD$_{100}$_120	120		97	3.1
PBA-co-PBT	ECOFLEX	70	54/46		2.4

In the following, the materials will be labelled as reported in Table 2.1. The *cis/trans* isomeric ratio was determined by the H NMR spectra, recorded at room temperature. Molecular weights were determined by gel permeation chromatography (GPC).

Methods

3.1. Calorimetric characterization

DSC analysis was carried out in order to investigate the effects of the polymer composition and molecular weight on the crystalline and amorphous phase. Tests were performed on crucibles contained approximately 10 mg of polymer. As shown in Figure 3.1, the DSC thermal history is constituted by two heating scans and one cooling scan, all at 10°C/min under a N_2 flow (50 ml/min). The temperature ranges, reported in Table 3.1, were defined according to data already reported in the literature (3) (6).
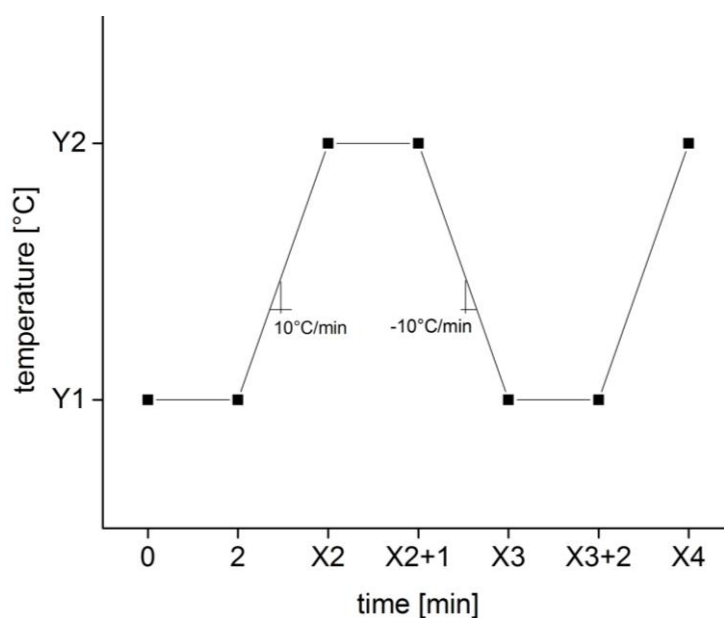
Figure 3.1 DSC thermal history applied to studied materials

Table 3.1 Temperature ranges for each Studied Materials

	PBA	PBA-PBCHD$_{100}$70/30	PBA-PBCHD$_{100}$50/50	PBCHD$_{100}$	ECOFLEX
Y1	-80°C	-70°C	-70°C	-30°C	-70°C
Y2	100°C	100°C	150°C	100°C	170°C

The first heating scan was performed in order to cancel the previous thermal history; thence the sample was kept at high temperature for 1 min and then cooled (cooling scan). During the cooling scan, the crystallization temperature (T_c) and the crystallization enthalpy (ΔH_c) were measured. After having reached the selected minimum cooling temperature, the sample was equilibrated at the temperature for 2 min and then heated (2nd heating scan). During the 2nd heating scan, the glass transition temperature (T_g), the melting temperature (T_m) and the melting enthalpy (ΔH_m) were determined as shown in Figure 3.2.
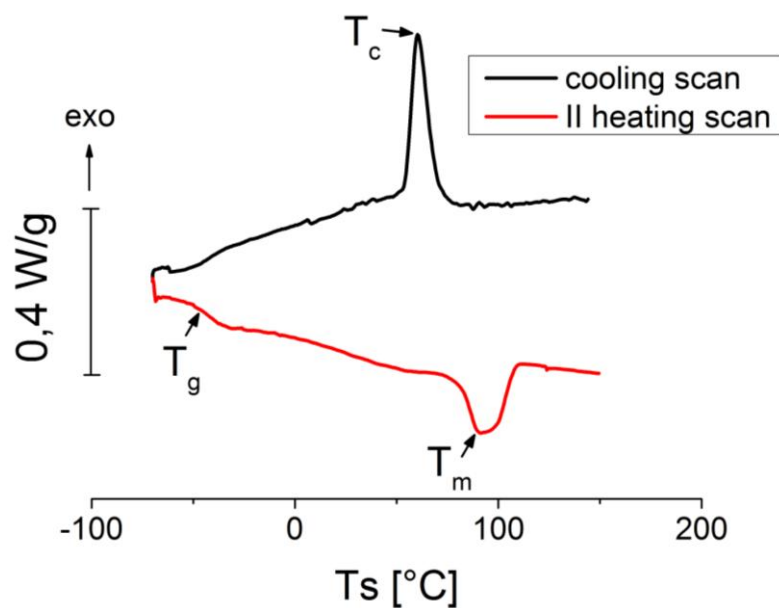
Figure 3.2 Cooling scan and second heating scan for PBA-co-PBCHD 50/50
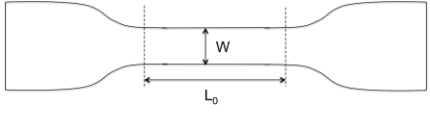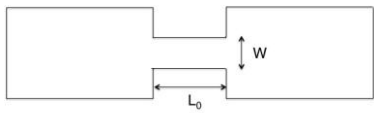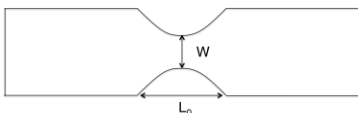
3.2. Tensile testing

Tensile testing was performed in order to characterize the mechanical behaviour of the materials, in particular their Young's Modulus and their behaviour at yield and at break.

3.2.1.   Specimens

To perform the tensile tests, three Dumbbell geometries were considered, as reported in Table 3.2.

Table 3.2 Dumbbell geometries used in tensile tests

TYPE	GAUGE LENGTH L_0 [mm]	MINIMUM WIDTH W[mm]	MINIMUM THICKNESS H[mm]	
DUMBBELL SAMPLE	33	6	1	
T SAMPLE	10	3	1	
TAPERED SAMPLE	14	2	1	

The measurement of the initial thickness of the specimen was obtained through a digital Mitutoyo micrometer with 0,001 mm sensitivity, while the width of the gauge length was measured through gauge with 0,02 mm sensitivity.

The Dumbbell shaped samples with gauge length of 30mm were used only to test the Ecoflex, which was the only material available in large amount. In this case the measurements for width and thickness were performed in three different points, in particular, two at the edges and one in the middle of the gauge length. The final measure was calculated as an average of the three.

On the contrary for the homopolymers and the copolymers PBA-co-PBCHD, the "T" shaped samples with gauge length of 10mm were used and the measurements for width and thickness were performed in a single point in the middle of the gauge length.

The third kind of sample, the tapered one, was used as test in order to verify that the behaviour of the material was not influenced by the geometry of the sample.

This having been verified the "T" specimens were chosen to perform the tensile tests since the measure of the strain is more precise on a constant gauge length.

3.2.2. Sample preparation

The specimens were obtained by punching compression of moulded sheets using a manual press. The sheets were moulded employing a compression moulding press. Two moulds with different sizes were used:

- 200x170mm^2 for fracture testing samples (thickness $\approx$ 0.5mm);
- 60x70mm^2 for tensile testing samples (thickness $\approx$ 1mm).

In order to obtain the desired thickness, the proper mass was determined assuming for all the materials a density similar to the Ecoflex one (1,26 g/cm^3) (1). The moulding process was carried out at 30°C above the T_m, determined by DSC, as shown in Table 3.3.

Table 3.3 Melting and molding temperatures of studied materials

MATERIAL	MELTING TEMPERATURE T_m [°C]	MOLDING TEMPERATURE [°C]
Ecoflex	124	160
PBCHD$_{100}$	165-171	200
(4-6)PBCHD$_{100}$ 50/50	94	120
(4-6)PBCHD$_{100}$ 70/30	53	85
PBA	52-57	90

In order to avoid the adhesion of the material to the mould, Bonnaflon© spray (PTFE spray) was laid on both sides of the mould.

The moulding cycle was the following: after the mould reached the mould temperature, the material was loaded and left into the mould for five minutes without pressure, in order to assure that all the material was molten; thence the mould was closed, a limited pressure was applied

and immediately cooled using cold running water, to avoid the runoff of the material, having a very low viscosity. The cycle ended when the mould was opened at different temperatures, varying between 25°C and 40°C, depending on each materials.

3.2.3. Equipment and testing conditions

The experiments were performed using a single column electromechanic dynamometer (Housfield) with a 5kN load cell, in a thermostatic lab with controlled temperature. Displacements along the gauge length were measured by the use of a mechanical extensometer.

The nominal stress was calculated as the ratio between the load and the sample cross-section:

$$\sigma = \frac{load}{Area_{cross\ section}} \tag{3.1}$$

The strain instead was measured as the ratio between the knives displacement and their initial distance:

$$\varepsilon = \frac{\Delta L - \Delta L_0}{6.25 + \Delta L_0} \tag{3.2}$$

where ΔL is the displacement measured in mm from the extensometer, ΔL_0 is the starting value (in mm) measured when the knives are positioned and varies for each test. 6.25 mm is the calibration distance at which $\Delta L_0 = 0$ mm.

As the first tested materials showed unexpectedly a brittle behaviour, the materials were suspected to be highly sensitive to notches that could be caused by the extensometer knives. To verify that the brittle behaviour did not depend on the kind of extensometer, other experiments were performed on an electromechanical INSTRON 1121 dynamometer, with 500 N load cell, employing a videoextensometer and its acquisition software VE500 for the measure of the displacement.

The measure of the strain was made using markers on the sample surface, which are detected by the videoextensometer. The strain was defined as the ratio between the difference of the markers positions along the y-axis and their starting distance:

$$\varepsilon = \frac{y_2 - y_1}{y_{02} - y_{01}} \tag{3.3}$$

The tests were performed in a thermostatic room at 23°C, under controlled relative humidity ($\leq$ 50%) and at atmospheric pressure. Moreover, different strain rates (0,000167 s^{-1}, 0,00167 s^{-1}, 0,033 s^{-1}) were applied in order to investigate also the effect of this variable

From preliminary data available to the research group of the University of Bologna (20), two main behaviours were expected, as reported in Figure 3.3.
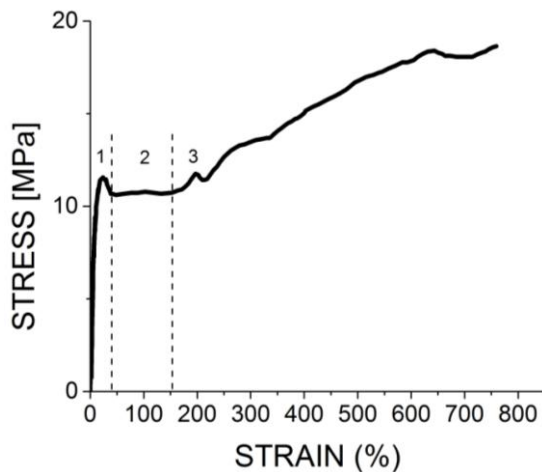
Figure 3.3 PBA-co-PBCHD 50/50 Stress VS Strain Curve
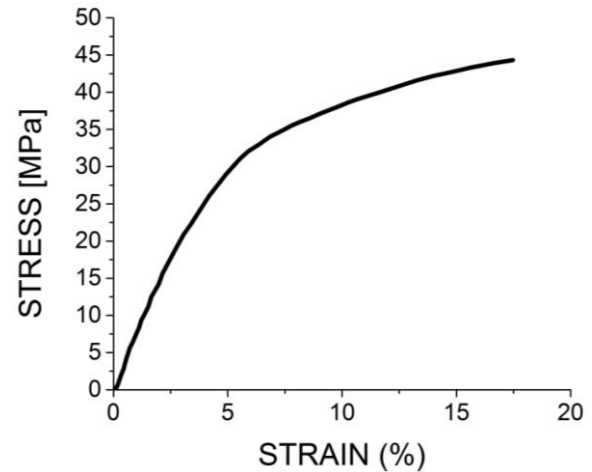
Figure 3.4 PBCHD Stress VS Strain Curve

In figure 3.3 is possible to identify three different regions:

1. Linear region and neck region, where yield occurs;
2. Cold drawing or plastic flow;
3. Strain hardening and break.

In this case, the Young's Modulus was determined as the slope of the stress-strain curve at strain below 1%, fitting the points of the curve in the linear region.

The values of strain and stress at yield, ε_y and σ_y respectively, were measured as the maximum point of the curve in the region where the necking occurs. On the same way, the behaviour at break is described by the stress and strain, σ_b and ε_b, observing the last point before that the load drops to zero value.

In case the behaviour is like that of Figure 3.4, only the first region can be observed and only the Young's Modulus and σ_b and ε_b can be determined.

3.3. Fracture tests

As said before, materials for packaging are usually in the form of thin films, thence it follows that it's important to characterize the fracture behaviour with a proper method. In this work the investigated material toughness was determined with the essential work of fracture method.

3.3.1. Specimens preparation

The fracture tests were performed on Double Edge Notched Tension (DENT) samples (19) (21) (22). The specimens were obtained by punching 0.5 mm thick films, obtaining rectangular samples of WxH=35x85mm^2. Also in this case films were compression moulded in the same condition as sheets for tensile testing. In this case, however, a bigger mould was used (200x170mm^2).
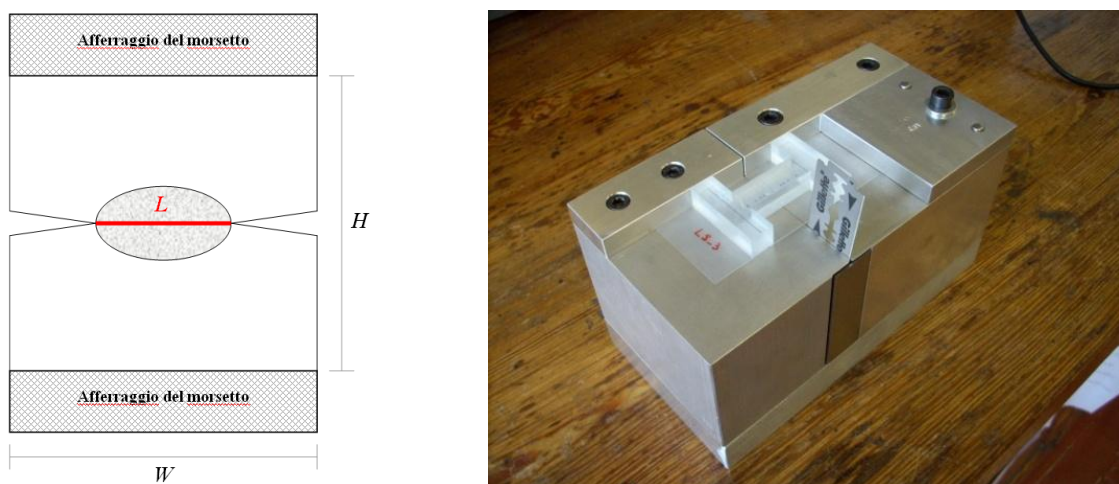
Figure 3.5 DENT sample and the punch used to obtain dent specimens

The notches were produced laying the polymer sheet on an aluminium base, equipped with H-shaped templates as end of stroke for the advancement of the blade. A razor blade was used to generate the notches, which resulted to have good alignment, small curvature radii and crack tip perpendicular to the specimen thickness.

As discussed before, since the available material was in few quantities, a statistical method, proposed by Steininger, was employed in order to reduce the number of samples and thus of the ligament lengths necessary to perform the tests, while maintaining the statistical validity of the method.

The Ecoflex samples were obtained with nominal ligament lengths of 5, 8, 10, 12 and 15 mm. The copolymer PBA-co-PBCHD$_{100}$ 70/30 was available in lower quantities, thus the nominal ligament lengths used were 5,10 and 15 mm; al least two tests were carried out for each ligament length. All the ligament lengths were measured with an optical microscope. Again, the specimen thickness was measured with a micrometer with 0.001 mm sensitivity was used. In order to check that yielding occurred before fracture starts, two markers were drown on the sample, opposite to each other with respect to the ligament, and at the same distance as the ligament length (Figure 3.6) (22) (23) (24) (25).
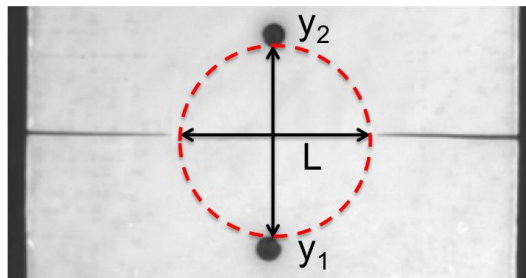
Figure 3.6 Markers drawn on a DENT sample

3.3.2. Equipment and testing conditions

All the fracture tests were performed with an electromechanical INSTRON 1121 dynamometer, with 500 N load cell, at 10 mm/min in a thermostatic room at 23°C, at controlled relative humidity (≤ 50%) and at atmospheric pressure. In order to measure the displacement and the strain a u-eye video camera was used to record the test at 6 fps or 10 fps. The recorded images were analysed by a macro program developed with the ImageJ software, which detects and measure the coordinates of the markers; as difference between the positions along the y-axis is possible to determine the displacement close to the process zone.

Results and discussion

In this paragraph all the results obtained during the calorimetric and the mechanical characterizations will be shown and discussed.

4.1. DSC analysis

First of all, the materials were characterized from a thermal and thermodynamic point of view, paying specific attention to the characteristic temperatures and to the enthalpy changes during the melting and crystallization process.

In the previous chapter "Method", the thermal history, carried out during the DSC analysis, was detailed. It is composed by two heating scans and one cooling scan, all at 10°C/min; the glass transition temperature and the melting temperature were taken from the second heating scan, but also the cooling scan was observed, in order to get a deeper insight of the thermal behaviour of the considered materials.
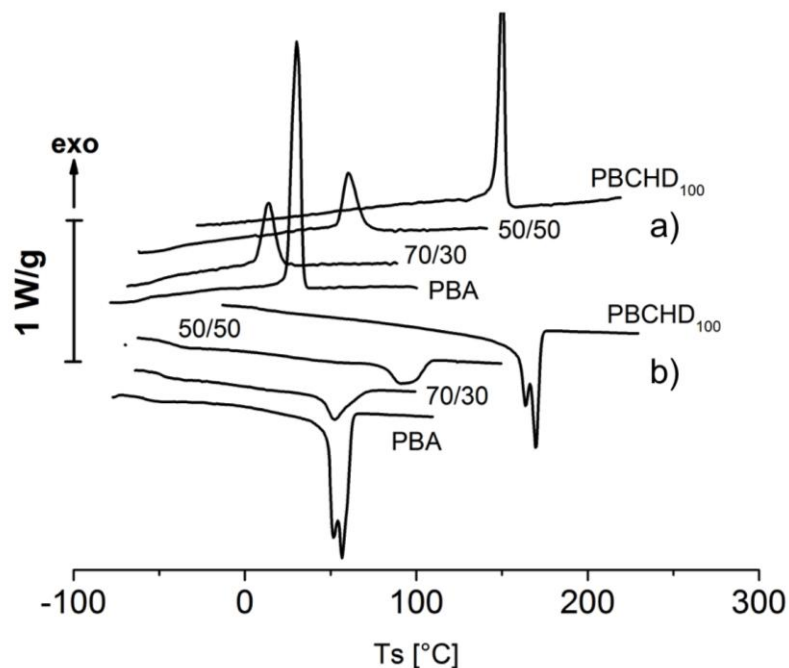
Figure 4.1 DSC traces obtained at 10°C/min during cooling from the melt (curves a) and during second heating (curves b) for all the materials with lower molecular weight

In Figure 4.1 the cooling scan and the second heating scan of the material with lower molecular weight are reported. First of all it is clear that all the materials have a crystalline phase, but it is also important to recall that, in the copolymers, only the $PBCHD_{100}$ crystallizes (6); moreover, as expected, the two homopolymers have very narrow and intense peaks, so they show a typical behaviour of polymers with high tendency to crystallize into perfect and stable crystals; the presence of a double peak, during the heating scan, was previously explained as a process of melting-recrystallization and remelting. Furthermore, for $PBCHD_{100}$, as disclosed in the introduction, the high percentage of trans isomer of the 1,4-cyclohexylene units allows the polymer to crystallize and to reach a relatively high level of crystallinity, indeed, for this material was not possible to determine the glass transition temperature. Also the copolymers show the ability to crystallize, but the peaks are larger and less intense. This suggests that in the copolymers the size distribution of the crystals is more scattered.

All the DSC curves are reported in appendix and, looking at them, it appears rather clearly that the characteristic temperatures do not change depending on the molecular weight; in support of this it's possible to observe the values shown in Table 4.1.

Table 4.1 Thermal data of the samples, the data marked by * are taken from (6) (20)

MATERIAL	Mw x 10^{-3}	T_g [°C]	T_m [°C]	T_c [°C]	ΔH_m [J/g]	ΔH_c [J/g]
PBA_49	49.1	-58	56.56	30.11	74	75
PBA_57	56.9	-58.52	57.67	29.65	58	54
PBA_90*	90	-58	57	32	70	67
70/30_58	58	-49	52.28	13.78	28	27
70/30_62	62	-52.49	54.88	20.68	33	31
70/30_95*	95.4	-49	53	14	24	28
50/50_40	39.6	-44	91.34	60.24	37	33
50/50_58	58.4	-40.49	97.87	55.73	29	28
50/50_64	63.9	-40.39	95.38	56.76	32	32
50/50_74*	73.6	-43	94	66	32	33
PBCHD$_{100}$_57	56.6		169.5	150.33	68	67
PBCHD$_{100}$_73*	73.4	10	171	149	42	43
PBCHD$_{100}$_83	82.6		170.43	142.264	51	60
PBCHD$_{100}$_120	120		168.025	137.05	55	58

As it is possible to observe, by comparing the experimental data with the literature one, the characteristic temperatures are consistent and do not change with the molecular weight. Only in the case of the crystallization temperature the data seem to be slightly scattered. In figure 4.2, 4.3 and 4.4, the characteristic temperatures for the materials with lower and higher molecular weights are shown as function of the BCHD content.
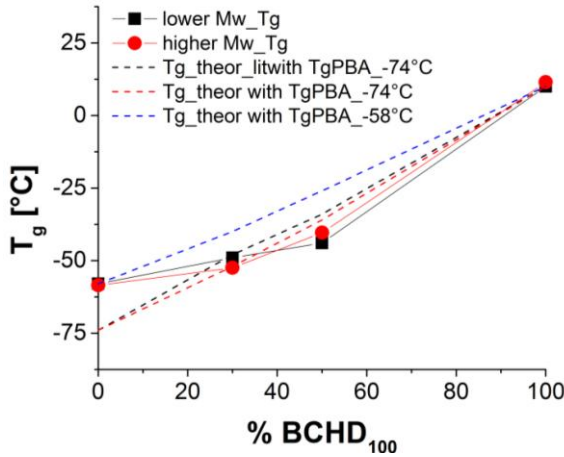
Figure 4.2 Trend of Tg values VS copolymer composition. symbols refer to experimental data and lines are the extrapolated curves obtained from the theoretical Tg data calculated by the fox equation
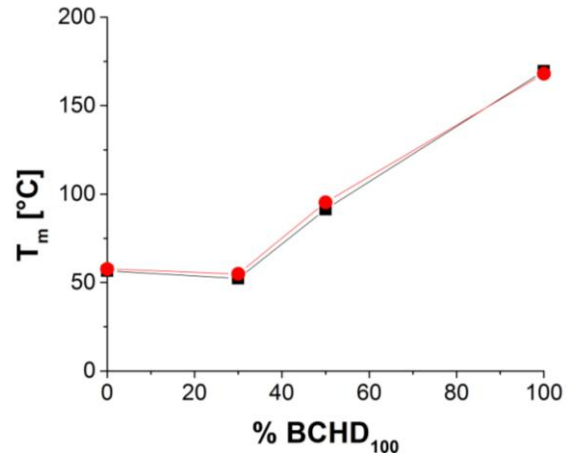
Figure 4.3 Trend of Tm values VS copolymer composition - II heating scan
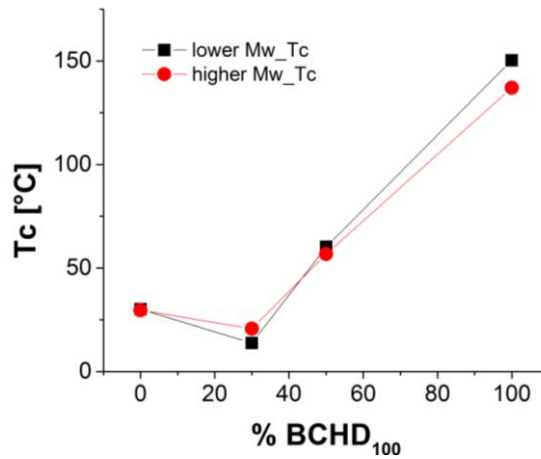
Figure 4.4 Trend of Tc values VS copolymer composition

For what concerns the glass transition temperatures in Figure 4.2 the experimental data are compared to the predictions of the Fox equation:

$$\frac{1}{T_{g\,FOX}} = \frac{w_1}{T_{g1}} + \frac{w_2}{T_{g2}} \tag{4.1}$$

where $T_{g\,FOX}$ is the calculated glass transition temperature of the copolymer, T_{g1} and T_{g2} are the glass transition temperatures of the two homopolymers, w_1 and w_2 their weight fractions in the copolymer.

Weight fractions were determined from molar fractions (N_1 and N_2) according to:

$$w_1 = \frac{N_1 MW_1}{N_1 MW_1 + N_2 MW_2} \tag{4.2}$$

$$w_2 = \frac{N_2 MW_2}{N_1 MW_1 + N_2 MW_2} \qquad (4.3)$$

where $MW_1 = MW_{BA} = 200$ g/mol, $MW_2 = MW_{BCHD} = 226$ g/mol and the effect of terminals are neglected.

Table 4.2 Theoretical Tg Data. a) weight fractions measured considering MW_{PBA}=200g/mol and MW_{PBCHD}=226 g/mol; b) Theoretical Tg values given from (6) (20) calculated with FOX Equation by using the tg value of the fully amorphous PBA sample, equal to -74°C (26) (27)

	$w_1 = w_{BA}$ [a)]	$w_2 = w_{BCHD}$ [a)]	T_g [b)] FOX LIT [°C]	T_g [c)] FOX [°C]	T_g [d)] THEOR [°C]
PBA-co-PBCHD$_{100}$ 70/30	0.6737	0.3262	-48	-53	-40
PBA-co-PBCHD$_{100}$ 50/50	0.4694	0.5305	-34	-37	-27

In literature (6) the $T_{g\ FOX}$ was evaluated considering for the PBA the value of T_g=-74°C, a value reported for the polymer in the fully amorphous state (26) (27). The reason of using this T_g value is that, in the copolymer, the PBA should be completely amorphous. However in Figure 4.2, three curves are shown, the black is that given by literature, the red uses the values recalculated using $T_{g\ PBA}$=-74°C and the blue is obtained using $T_{g\ PBA}$=-58°C, the experimental value found in this work for PBA. As it is possible to observe the experimental data are slightly lower than the theoretical ones.

Coming to the crystalline phase, a continuous decrement in crystallization temperature with the decrement of BCHD unit content is evident (Figure 4.4). It is worth considering that the melting temperatures of the two copolymers is closer to the PBA one than to the PBCHD$_{100}$ one, even if the crystalline phase is expected to be composed only by the latter (6).

Moreover, also the melting and crystallization enthalpies have been evaluated in order to verify if they change with the molecular weight and to make some considerations on the crystalline phase of the copolymer. In Figure 4.5 a) b) c) and d) the melting and crystallization enthalpies are shown as function of the molecular weight for each material. From these data, the effect of molecular weight is negligible in the case of copolymers, while in the case of the homopolymers the enthalpies seem to show a dependence on molecular weight. However, as the calorimetric curve of Figure 4.1, show multiple peaks on heating and broad tail at temperatures lower than Tc on cooling, some doubt arise about the precision in determining ΔH values. Moreover a non-

monotonic trend is difficult to interpret. A deeper investigation, testing a wider number of molecular weights, should be carried out.

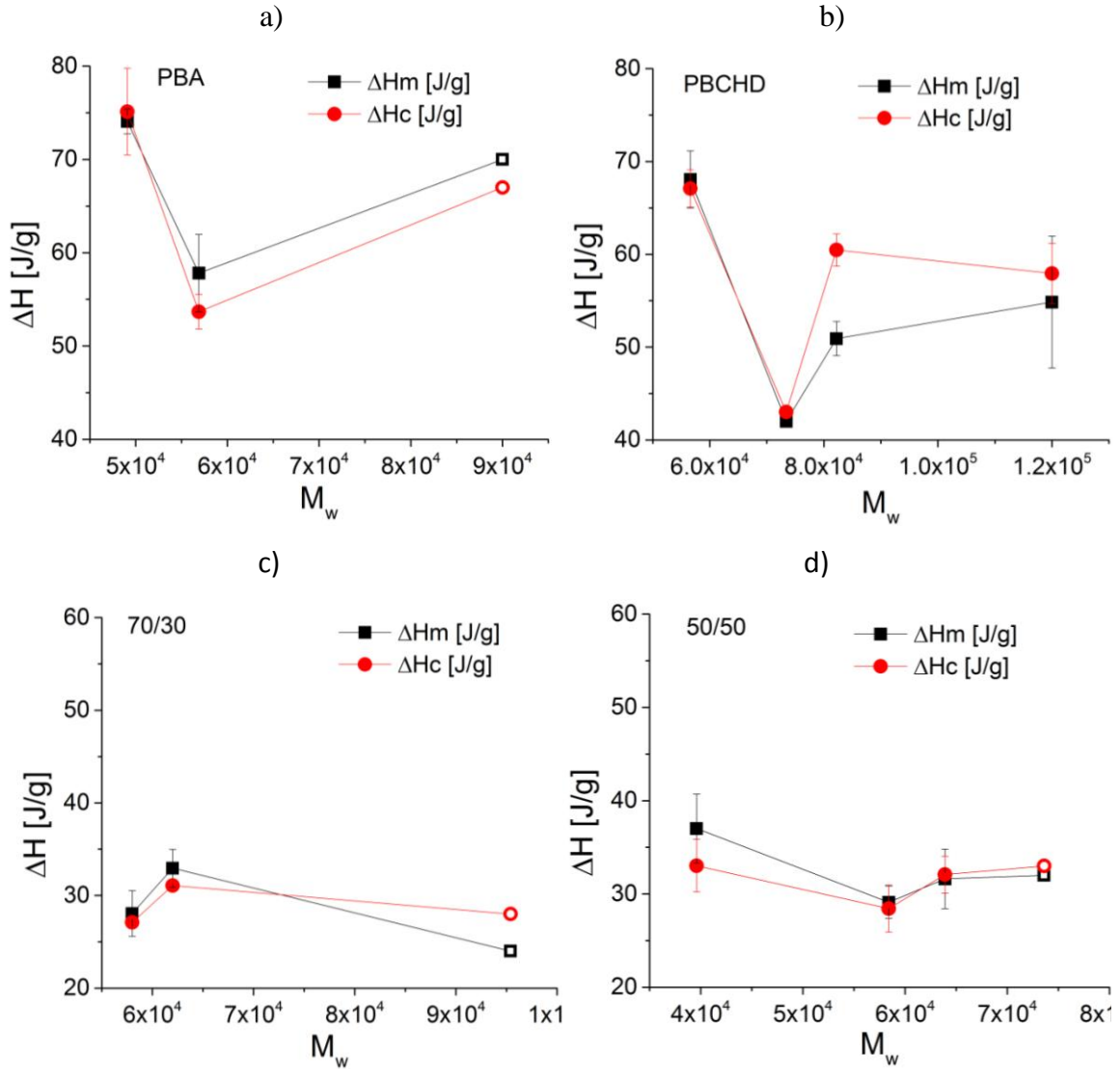**Figure 4.5 Melting and crystallization enthalpy as function of molecular weight for a)PBA, b)PBCHD, c) Copolymer 70/30, d) Copolymer 50/50**

In Figure 4.6 and Figure 4.7 it is possible to observe the enthalpies of melting and crystallization as function of the BCHD content for materials with M_w around 60000. The trend reported for the specific case seems valid also for the other available molecular weights.
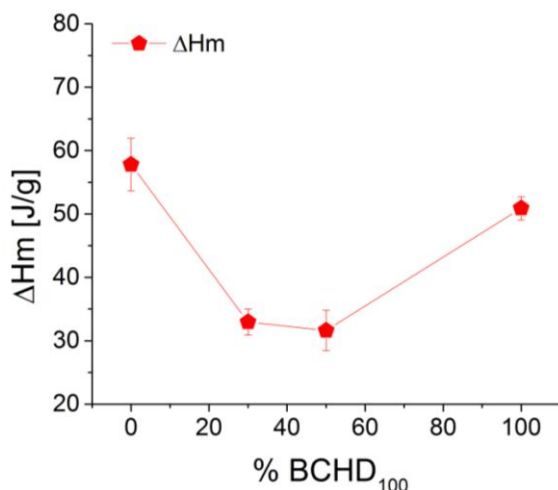
Figure 4.6 Melting Enthalpy as function of PBCHD content at M_w around 60000
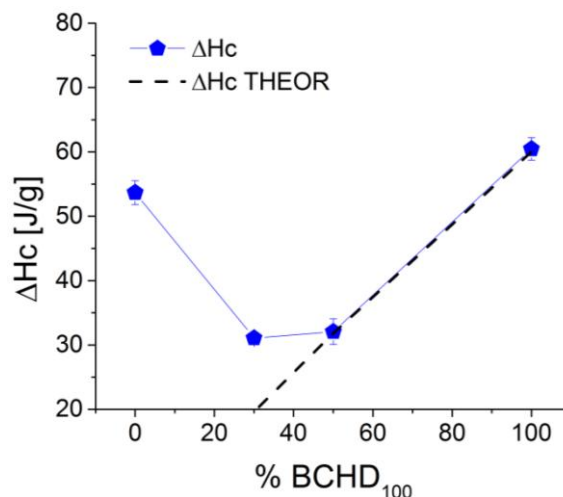
Figure 4.7 Crystallization Enthalpy as function of PBCHD content at M_w around 60000

Comparing the values for ΔH_m e ΔH_c, it can be observed that they slightly differ: in literature (6) this difference is attributed to the melting-crystallization-remelting process, which occurs only during the heating and not during the cooling scan. More likely, this difference may be due to the aforementioned troubles in determining the base line and bounds of the crystallization peak.

In Figure 4.7 in addition to the experimental data, the reported black line highlights the expected values of the crystalline enthalpies, measured multiplying the $\Delta H_{c\ PBCHD}$ by the BCHD content, and, as can be observed, the experimental value of the copolymer 70/30 is really higher than the expected one.

Focussing on crystallization, in literature (6) it was reported that the crystalline phase should be constituted only by the $BCHD_{100}$, thence the mass of BCHD forming the crystal is independent on the copolymer composition. Should it be true, the ΔH_c should decrease linearly with BCHD content, which, from Figure 4.7, is true only in the case of the 50/50 copolyester. This is further illustrated in Figure 4.8 where the crystallization enthalpy is referred to the mass of BCHD: it can be observed that in the case $PBCHD_{100}$ and PBA-co-$PBCHD_{100}$ 50/50 copolymer the enthalpy is the same, this suggesting the conclusion reported in literature, while in PBA-co-$PBCHD_{100}$ 70/30 copolymer it is higher. In this case, also BA seems to crystallize. The interesting fact that WAXD analysis in (6) shows only features typical of PBCHD crystalline phase suggests the hypothesis of a co-crystallization. However, this should be further investigated.
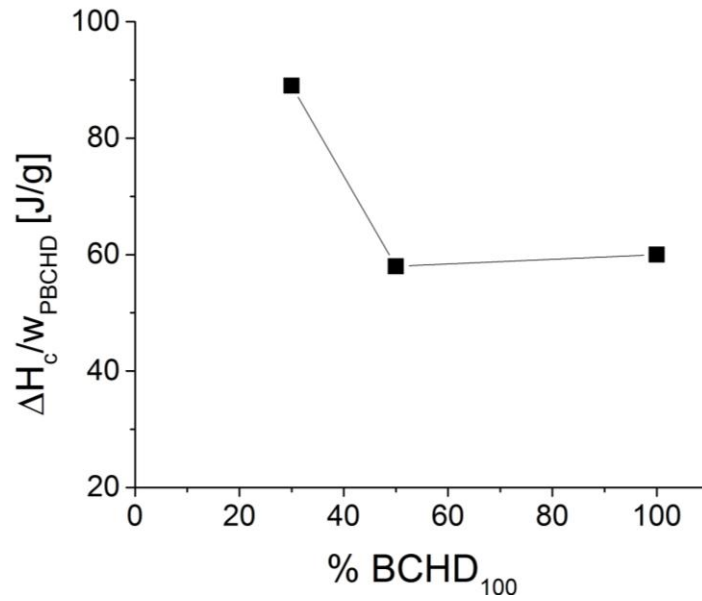
Figure 4.8 Crystallization Enthalpies normalized on PBCHD$_{100}$ content as function of the composition

From the calorimetric analysis it appears that the copolymer crystalline phase is always constituted by the same mass amount of BCHD and only in the copolymer PBA-co-PBCHD$_{100}$ 70/30 also by an unknown quantity of BA, while the amorphous phase is mainly constituted by BA. This structural hypothesis will be discussed in the following chapters in the light of the experimental data obtained by the mechanical characterization.

4.2. Tensile tests

The tensile tests were carried out on all the materials, including Ecoflex. From preliminary tests (20) all materials show a maximum in the stress-strain curve, which is arbitrarily identified with yielding, followed by plastic flow and strain hardening, with the exception of the $PBCHD_{100}$, which breaks immediately after yielding. Next, some of the obtained curves and the extracted properties, such as the Young's modulus, the stress and stain at yield and at break are reported.

4.2.1.   Ecoflex
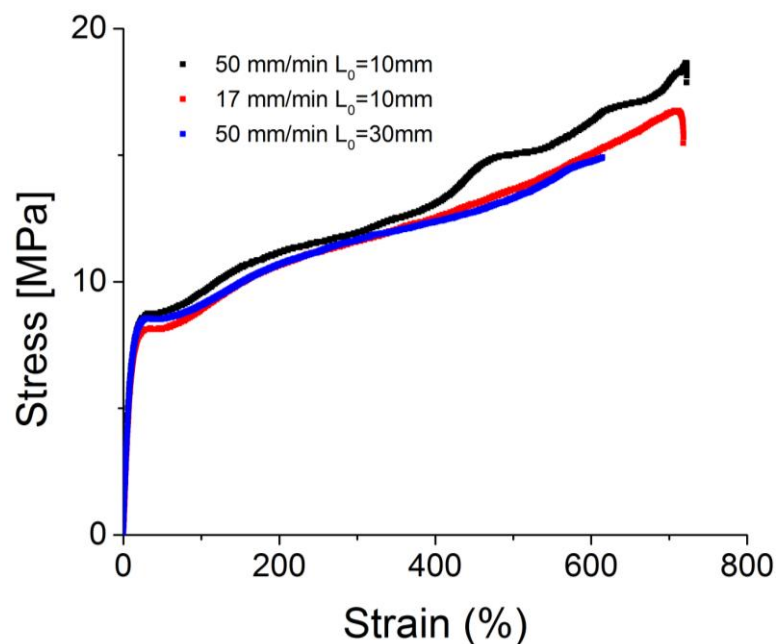
Figure 4.9 Ecoflex Stress-Strain curves at different strain rates

The stress-strain curves, shown in Figure 4.9, were obtained from different geometries and at different displacement rates. To be more precise the black and the red curves were obtained employing a "T" specimen, respectively at $0,0833s^{-1}$ and $0,0283s^{-1}$, instead, the blue one, employing a Dumbbell specimen at the same strain rate as the red. It is also possible to observe that in the last case the material did not break before the maximum displacement allowed from the dynamometer was reached. From a set of tests a mean value of the Young's Modulus and of the stress and strain at yield and at break was measure (Table 4.3) and are reported along with data from preliminary tests.

Table 4.3 Ecoflex mechanical properties obtained from four samples for each material

	YOUNG`S MODULUS [MPA]	STRAIN AT YIELD %	STRESS AT YIELD [MPA]	STRAIN AT BREAK %	STRESS AT BREAK [MPA]
	69±4	31.6±2.9	8.5±0.3	766±138	17.34±1.4
LIT	67.8±7.9	36±2.9	8.4±0.9	1204±264	17.9±2.6

As the test conditions and methods for preliminary data era unknown, no conclusions can be drawn from the comparison between the preliminary (20) and the present data. However, it can be observed that they are at least, consistent. In particular the Young's Modulus and the stress at yield and at break are included into the statistic error of the preliminary tests. The strain, instead, is slightly lower than the preliminary value, both at yield and at break. As for the effect of the strain rate on the stress at yield, it does not seem considerable. It should be however observed that the strain rate range considered is rather limited.

4.2.2. PBA
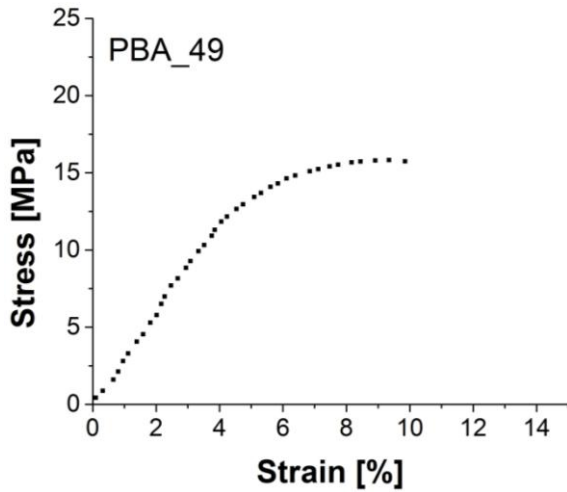
Figure 4.10 PBA_49 Stress-Strain curves
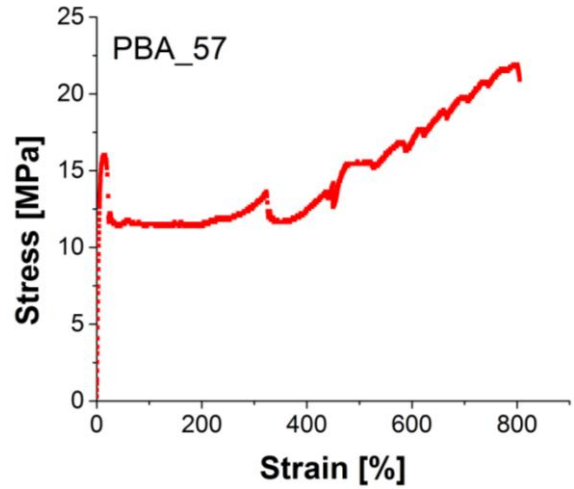
Figure 4.11 PBA_57 Stress-Strain curves

When PBA is considered, some findings have to be highlighted. First of all, an effect of molecular weight is observed: indeed, PBA_57 (Figure 4.11) shows the expected ductile behaviour, similar to that observed in the preliminary work on a sample with M_w=90000 (PBA_90), and exhibits the three regions discussed before, a linear region, where the Young's Modulus is measured, followed by the yielding process, a region where the plastic flow occurs and in the last region there is the strain hardening. The PBA_49, on the contrary, shows a relatively more brittle behaviour and breaks before the maximum of the stress-strain curve, taken arbitrarily as yield point. A second remark has to be done about the several peaks observed in Figure 4.11. These seem to be associated to the occurrence of several, localized "necking" on the sample, as justified by the change in strain rate measured by the extensometer on the sample (Figure 4.12).
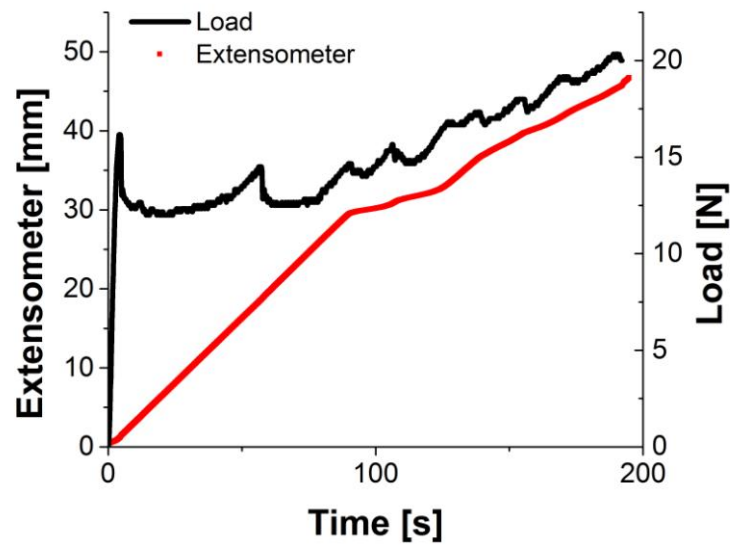
Figure 4.12 Load and Extensometer trend as function of Time to observe if the strain rate changes according to the load peaks

However, no inhomogeneity could be directly observed during the tensile tests and all the samples appeared to deform homogeneously. A deeper analysis of the phenomenon could have been carried out but due to a lack of material it was not possible.

Table 4.4 PBA mechanical properties obtained from four samples for each material

	YOUNG'S MODULUS [MPA]	STRAIN AT BREAK %	STRESS AT BREAK [MPA]	STRAIN AT YIELD %	STRESS AT YIELD [MPA]
PBA_49	338.3±49	9.67±0.3	15.5±0.3	0	0
PBA_57	254±1.8	737±89	19.9±2.8	12.75±2.5	15±1.3
PBA_90*	295.2±13.7	601.9±17.9	18.9±1	19.6±0.6	19±0.5

4.2.3. PBA-co-PBCHD$_{100}$ 70/30
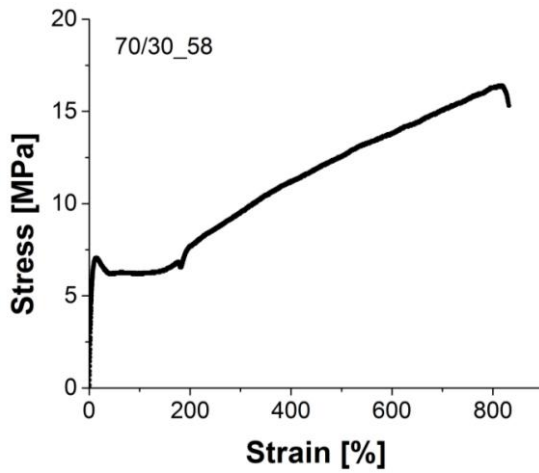
Figure 4.13 70/30_58 Stress-Strain curves
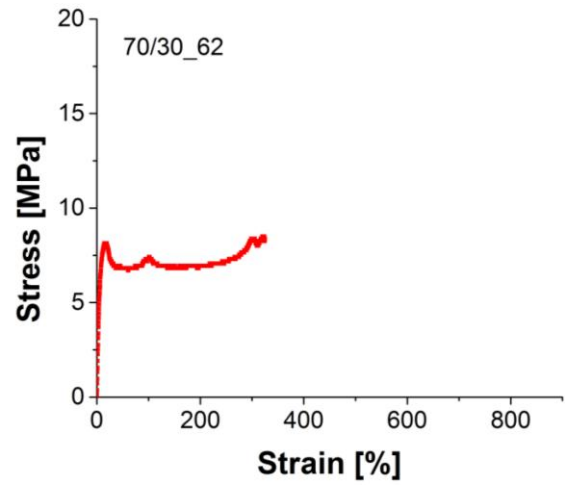
Figure 4.14 70_30 Stress-Strain curves

In the case of the copolymer 70/30 both the materials show a ductile behaviour, more ductile for the 70/30_58, whose curve presents the four different regions described for the PBA. The copolymer 70/30_62, instead, seems to reach the break immediately after the plastic flow, with very limited strain hardening. The yielding values and the Young's Modulus for the two molecular weights are comparable, while the values at break are lower in the case of 70/30_62 (Table 4.5). Unfortunately there are not literature values in order to make a comparison.

Table 4.5 70/30 Copolymers Mechanical Properties obtained from four samples for each material

	YOUNG'S MODULUS [MPA]	STRAIN AT BREAK %	STRESS AT BREAK [MPA]	STRAIN AT YIELD %	STRESS AT YIELD [MPA]
70/30_62	115±8.9	211.5±150	7±2.3	14.2±3.7	7.8±0.3
70/30_58	124.6±16.5	796.5±31.7	15.7±0.5	14.8±1.2	6.9±0.2

4.2.4. PBA-co-PBCHD$_{100}$ 50/50

Figure 4.15 50/50_40 Stress-Strain curves
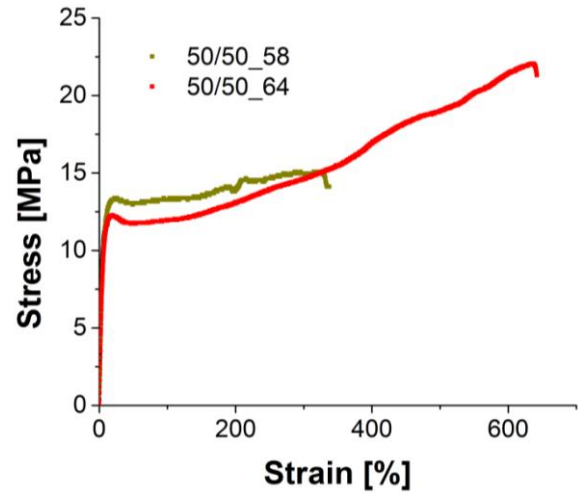
Figure 4.16 50/50_58 AND 50/50_64 Stress-Strain curves

For the copolymer 50/50 three materials, with different molecular weight, were available and as can be observed in Figure 4.15 and Figure 4.16 the behaviour changes significantly. The 50/50_40 shows a relatively brittle behaviour, on th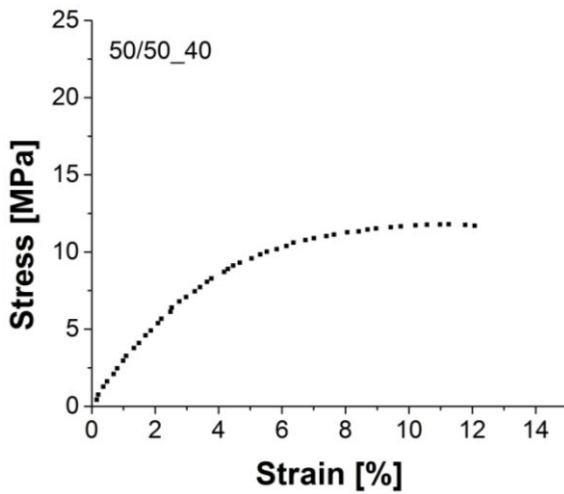e contrary the other two material, 50/50_58 and 50/50_64, show a ductile behaviour. In the latter material the strain hardening region extends to significantly higher strain. The Young's modulus is similar for all materials and the experimental values obtained are higher than those given in previous work on copolymer with M_w=74000. As for the case of PBA_49, for the 50/50_40 all samples break before the maximum in stress strain curve.

Table 4.6 50/50 Copolymers Mechanical Properties obtained from four samples for each material

	YOUNG'S MODULUS [MPA]	STRAIN AT BREAK %	STRESS AT BREAK [MPA]	STRAIN AT YIELD %	STRESS AT YIELD [MPA]
50/50_40	202.9±3	9.6±3.7	10±2.9	0	0
50/50_58	172.5±29.5	317.2±71.8	14.8±0.6	24.6±1.2	12.78±0.6
50/50_64	200±3.8	637±9.3	22±0.15	20.7±2.6	12.3±0.05
50/50_74*	143.1±10.7	710.6±174.6	18.9±1.6	24.9±1.8	12.1±0.8

4.2.5. PBCHD100
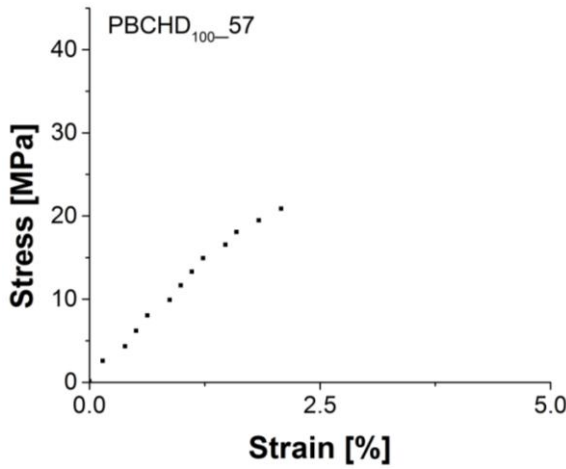
Figure 4.17 PBCHD_57 Stress-Strain curves
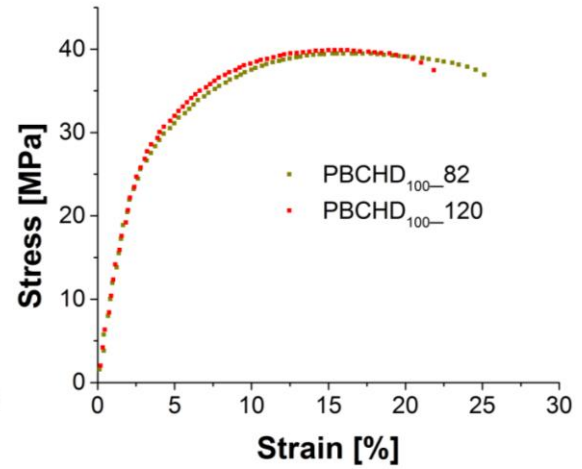
Figure 4.18 PBCHD_82 and PBCHD_120 Stress-Strain curves

Finally the $PBCHD_{100}$, instead, displays a relatively brittle behaviour for all the available molecular weights, even if at increasing M_w the material becomes more ductile (Figure 4.18) and a maximum in the stress strain curve can be observed. No plastic flow and strain hardening occur. By comparing the data with previous work preliminary tests (20), the Young's modulus is always higher than reported and, as said before, it can be justified since the test conditions and the method to gauge the strain are unknown.

Table 4.7 PBCHD$_{100}$ Mechanical Properties obtained from four samples for each material

	YOUNG'S MODULUS [MPA]	STRAIN AT BREAK %	STRESS AT BREAK [MPA]
PBCHD$_{100}$_57	1109.8±62	2.38±0.4	23.7±2.5
PBCHD$_{100}$_73*	727±89	18±3.8	40.9±3.6
PBCHD$_{100}$_82	1114.95±97	23.84±4.6	35.9±1.8
PBCHD$_{100}$_120	1005.8±110	19.77±4.3	37.47±1.3
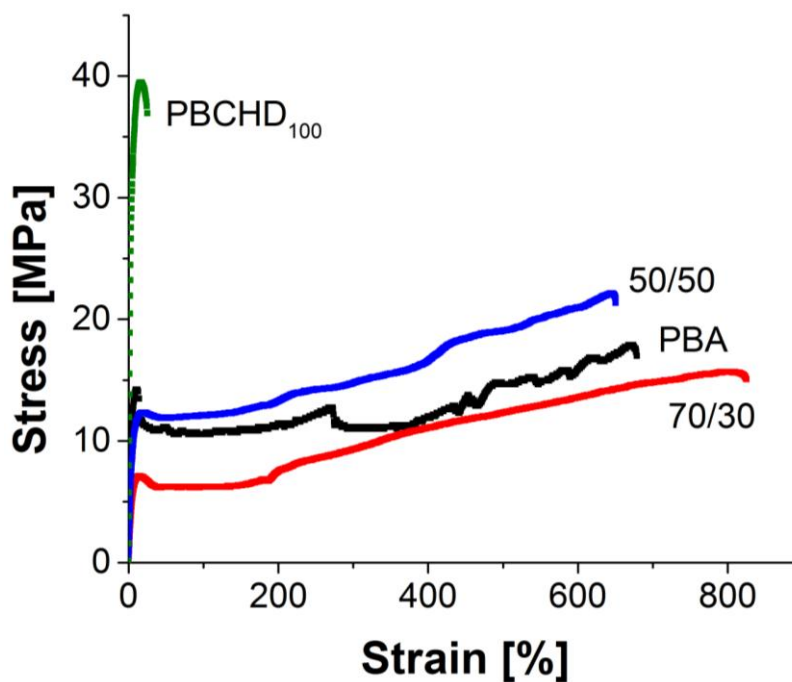
Figure 4.19 Stress-Strain curves for all the materials

In Figure 4.19 the stress-strain curves for each tested material are shown; it is possible to observe that the $PBCHD_{100}$ reaches values of stress significantly higher than the other materials, nevertheless it breaks before the plastic flow occurs. On the contrary the PBA and the other copolymers reach very high values of strain and the stress at break decreases from about 40 MPa to 20 MPa and then 12 MPa as the content of BA-units in copolyesters increases from 0 to 70%. This is a logical consequence of decreasing of rigid $BCHD_{100}$-units in copolymers.

4.2.6.   Effect of molecular weight on mechanical response

As analyzed before, in all the considered homo- and co-polymers, significantly different behaviours were observed. As all the samples were processed and tested at the same conditions, the difference can be ascribed to the molecular weight. Therefore the effect of this variable is worth further consideration.
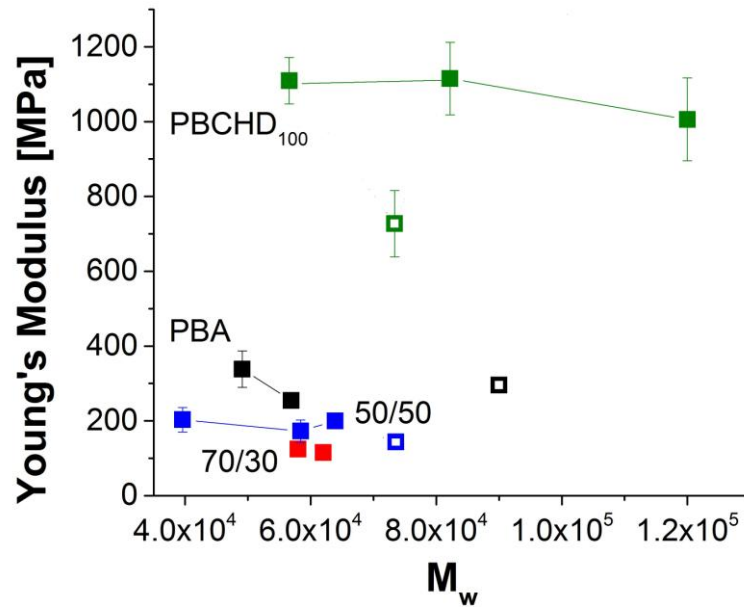
Figure 4.20 Young's Modulus as function of Mw, the empty points are from (20)

Starting from the observation of the Young's Modulus, in Figure 4.20 it can be expected that behaviour at low strains is independent on the molecular parameter. Indeed no correlation between Young's Modulus and M_w can be observed (Figure 4.20). The only value that differs significantly is the PBCHD$_{100}$ empty point, which is taken from preliminary work (20). As said before, the test conditions and how the strain was measured in this case are unknown. If the strain is measured from the crosshead displacement and not through the extensometer, the Young's Modulus results significantly lower; indeed, in order to measure the Modulus, the crosshead compliance should be taken into account and measurement chain can be described as a series model, where the apparent Modulus is given by a contribution due to the crosshead and a real contribution due to the material:

Figure 4.21 Series model

$$\sigma = \varepsilon E_{apparent} = (\varepsilon_{crosshead} + \varepsilon_{material})E_{apparent}$$

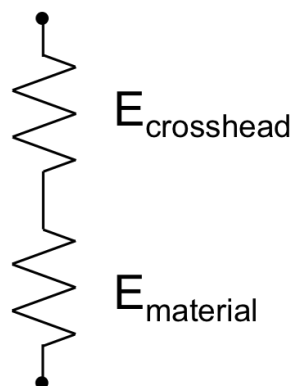$$= \sigma \left(\frac{1}{E_{crosshead}} + \frac{1}{E_{material}} \right) E_{apparent} \tag{4.4}$$

$$\frac{1}{E_{apparent}} = \frac{1}{E_{crosshead}} + \frac{1}{E_{material}} \tag{4.5}$$

Should it be the case, the modulus measured in preliminary tests might be the apparent one, which is expected to be lower than the material's one. Moreover, the underestimation should be more significant for the case of a stiff material, as the $PBCHD_{100}$.

While the molecular weight does not seem to affect the deformation mechanisms at low strains, it can be expected that behaviour at high strains is dependent on this molecular parameter, allowing yielding followed by plastic flow only above a certain threshold.
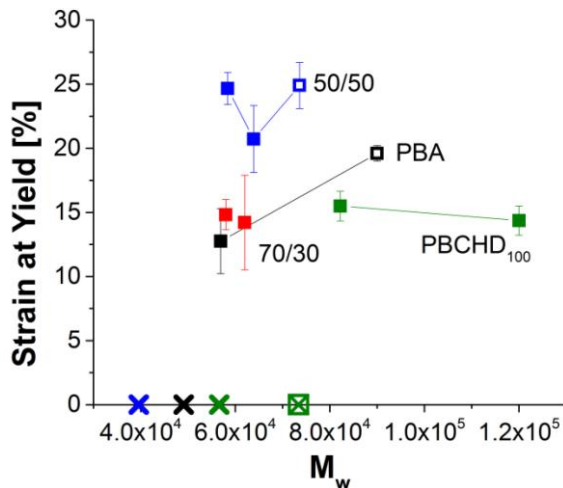

Figure 4.22 Strain at Yield as function of molecular weight. crosses represent samples that do not show nor yielding (maximum in stress-starin curve) neither plastic flow. empty points represent data from prelimnary tests (20)
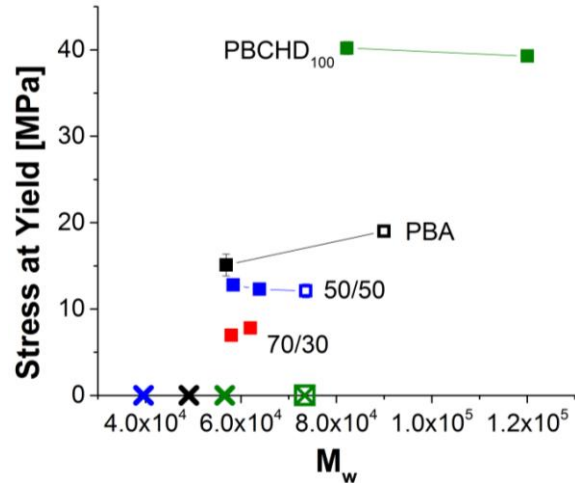
Figure 4.23 Stress at Yield as function of molecular weight. crosses represent samples that do not show nor yielding (maximum in stress-starin curve) neither plastic flow. empty points represent data from prelimnary tests (20)

For what concerns the strain and stress at yield, some different considerations can be made. As it is possible to observe from Figure 4.22 and Figure 4.23, below a certain molecular weight value the homopolymer PBA and the copolymer 50/50 do not reach a maximum, thus the stress and strain at yield cannot be measured and the plastic flow does not occur. Above this threshold molecular weight a very limited increase –if any- at increasing molecular weight can be observed for strain at yield, while stress at yield seems unaffected by M_w. In $PBCHD_{100}$ the plastic flow phenomenon never occurs, nevertheless above a threshold value ($M_w \approx 75000$), higher respect to the other materials ($M_w \approx 60000$), a maximum in stress strain curve is reached but the samples break before plastic flow; on the contrary, below that threshold value the material is more brittle and the maximum is not reached.

As the considered materials are semicrystalline polymers, tested at a temperature between Tg and Tm, a model to interpret the mechanical behaviour is that reported by Stroble, according to which, there exists four different phenomena responsible for permanent deformation: the onset and development of isolated inter- and intra-lamella slip processes (Figure 4.24 A), a change into a collective activity of slips (Figure 4.24 B), the beginning of crystallite fragmentation (Figure 4.24 C) and, finally chain disentaglement (Figure 4.24 D) (28) (29) (30). This phenomena occurs at critical (true) strain values during tensile tests and can be associated, as sketched in Figure 4.24 to the different phases of the stress-strain behaviour.
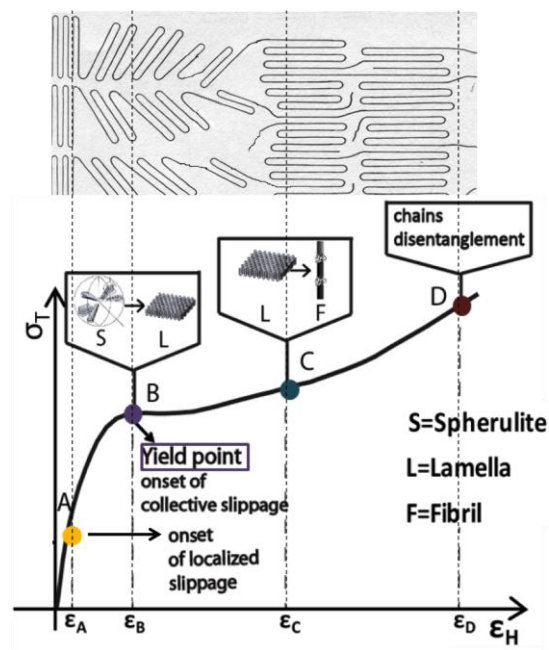

Figure 4.24 Deformation Mechanisms in Semicrystalline polymers (31)

It can be assumed that in order to have the collective activity, the stress can be transferred to the spherulites by the amorphous phase, through tie molecules and entanglements. However, should the molecular weight be limited, the tie molecules and entanglements density might be too limited to favour this collective phenomenon. This seems to be the case of PBA. As the same phenomenon is observed also for the copolymer, it may be concluded the BA – which is the most abundant component in amorphous phase from DSC analysis – is the responsible of the phenomenon.

Considering the behaviour at break, in Figure 4.25 and Figure 4.26 both the strain and stress at break are normalized with respect to their minimum value, in order to verify if a trend can be defined. The star shaped points, at value 1 of stress and strain, are obtained for materials with molecular weight below the threshold, which break after yielding and do not show plastic flow. In the case of PBA-co-PBCHD$_{100}$ 70/30, both the two materials available show plastic flow and

strain hardening and reach values of strain at break comparable, as it can be observed in Figure 4.25. The empty points represent the preliminary values.
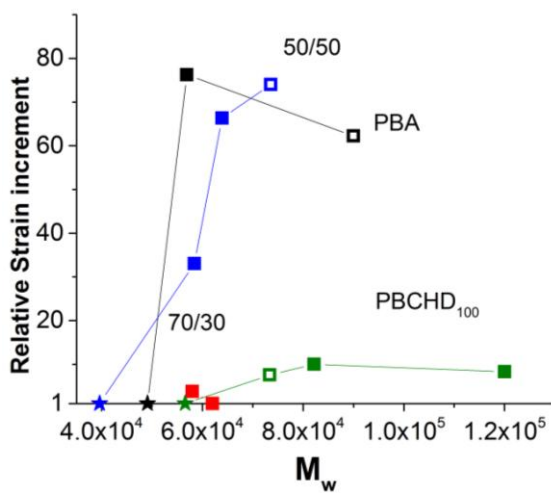

Figure 4.25 Strain for each material normalized with respect to the lower value as function of the molecular weight
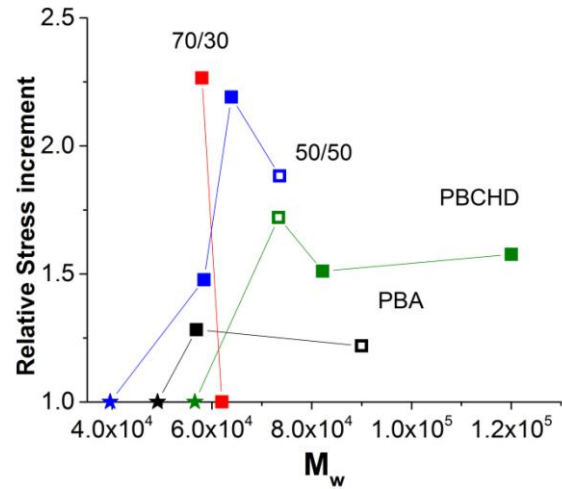
Figure 4.26 Stress for each material normalized with respect to the lower value as function of the molecular weight

Looking at the figures, a very significant increase in strain at break can be observed for all the materials going from the lower molecular weight, where the behaviour is relatively brittle towards higher ones. After an initial jump, the increase seems to level-off, even if this conclusion should require a further investigation.

Compared to the effect on strain at break, the M_w effect on stress at break is more limited, but still observable. Again, stress at break increases significantly when the molecular weight increase allows collective activity of inter- and intra-lamellar slips and the following deformation mechanisms. When M_w is higher enough to favour these phenomena the effect of M_w seems to be less significant.

The only exception to the general trend is the 70/30 copolymer, for which the effect of the two (indeed quite close) M_w seems negligible on the strain at break and even negative on the stress at break. However, more testing should be performed to confirm these results.

To sum up, for all materials an increase in M_w seems to favour the deformability. While PBCHD$_{100}$ displays a relatively brittle behaviour for all the investigate range of molecular weight, in the case of PBA and copolymers an M_w threshold exists, after which plastic flow can occur. This observation is in agreement with those form calorimetric analysis, according to which PBA in the copolymer is the amorphous phase, and should expected to be responsible for plastic deformation mechanism when yielding occurs, at least for the copolymer 50/50. The 70/30 would require a deeper investigation.

4.2.7. Effect of composition

Figure 4.26 reports the Young's Modulus as a function of BCHD content; recalling that the crystalline phase is constituted mainly by the $BCHD_{100}$ and the amorphous by the BA, the modulus follows the expected trend, decreasing as the $BCHD_{100}$ content decreases; nevertheless in the copolymer PBA-co-$PBCHD_{100}$ 70/30, the modulus does not decrease such as expected: this may occur since, as discussed previously, in the copolymer 70/30 also the BA takes part to the crystalline phase.
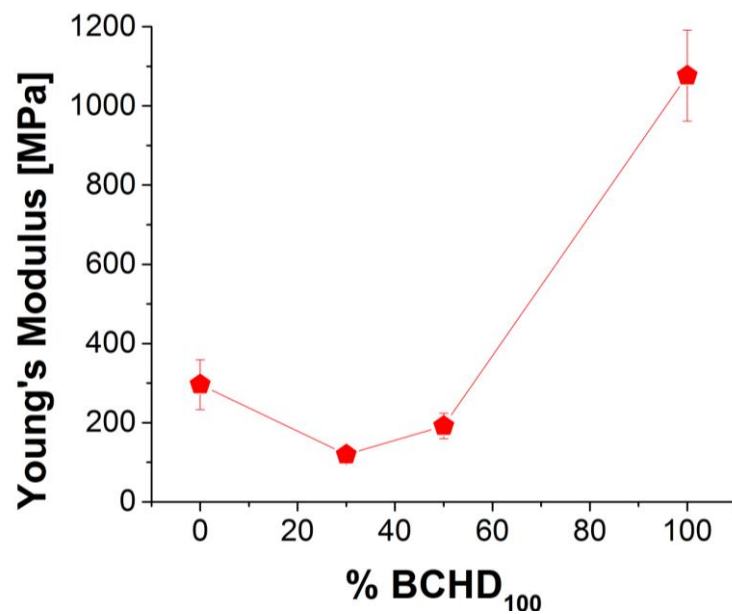

Figure 4.27 Mean values of young's modulus for the materials with different molecular weight as function of PBCHD content

Studying the effect of composition on the behaviour at yield and at break is tricky, as a significant effect of molecular weight has been discussed and no data with the same M_w are available. However, the molecular weight effect was observed to be less significant after a threshold that from Figure 4.22 seems of the order of $50x10^3$. Thus a rough comparison can be attempted for materials with M_w around to 60000. This is reported in Figure 4.28 and Figure 4.29 for yielding and Figure 4.30 and Figure 4.31 for break. In all the following figures, for what concerns the copolymers two different points are shown, since there where two materials with M_w around 60000, more precisely the red points represent the materials 70/30_58 and 50/50_58 and the black ones the 70/30_62 and 50/50_64.
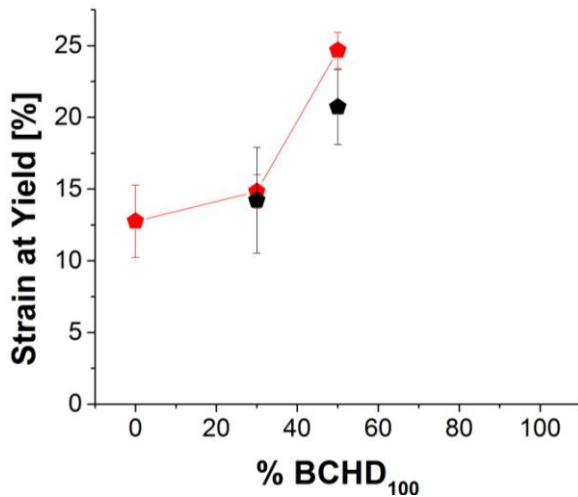
Figure 4.28 Strain at yield for materials with mw around 60000 as function of PBCHD content
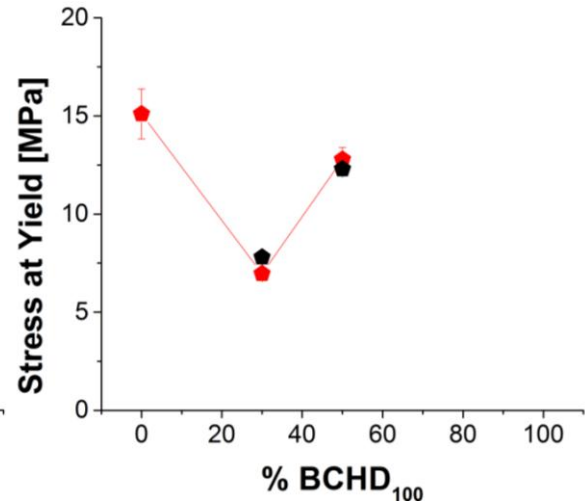
Figure 4.29 Stress at yield for materials with mw around 60000 as function of PBCHD content

In Figure 4.28 and Figure 4.29, the behaviour at yield is shown. The PBCHD values at yield are not shown since its molecular weight threshold is higher than 60000, about 75000 and below this value yielding does not occur. As for the strain at yield, an increasing trend with BCHD content can be. As BCHD constitutes mainly the crystalline phase, the effect should be related to the different BA content. However in the work it was not possible to estimate the amount of BA, as it enters in the crystalline phase for both PBA and 70/30 copolymer. From the data, showing an higher deformability before yielding at increasing BCHD content it seems that the BA content in amorphous phase increase as well, but this is just an hypothesis which would require a careful check. As for the yield stress, it can be observed to scale in a similar manner of Young modulus, and its trend might be explained in similar fashion.

In Figure 4.30 and Figure 4.31, instead, it is possible to observe the behaviour at break. As for strain at break, it show a general decrease at increasing BCHD content. The PBCHD displays a very low value due to the lack of collective activity of inter- and intra-lamella slips for the selected M_w. No clear trend can be observed for stress at break. However, these observations cannot be related with any consideration about material structure and deformation mechanisms, firstly because the strain measurement here adopted is not "local" enough to draw sound conclusion on the strain at break, and then because the rupture is probably caused by random imperfections in the sample.
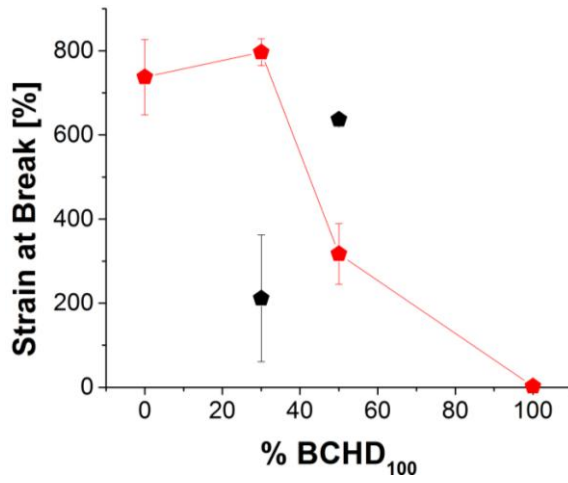
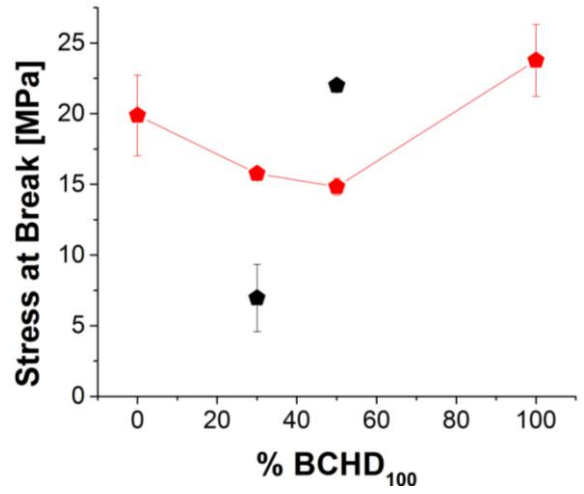**Figure 4.30 Strain at Break for materials with mw around 60000 as function of PBCHD content**

Figure 4.31 Stress at Break for materials with mw around 60000 as function of PBCHD content

4.3. Essential Work of Fracture

The essential work of fracture was measured on two different materials, the Ecoflex and the copolymer PBA-co-PBCHD 70/30, since they were the only materials available in sufficient amount.

4.3.1.   Ecoflex

As discussed in the "Materials and Methods" chapter, on the Ecoflex were carried out at least two tests at 5 different ligament lengths (5, 8, 10, 12 and 15 mm).
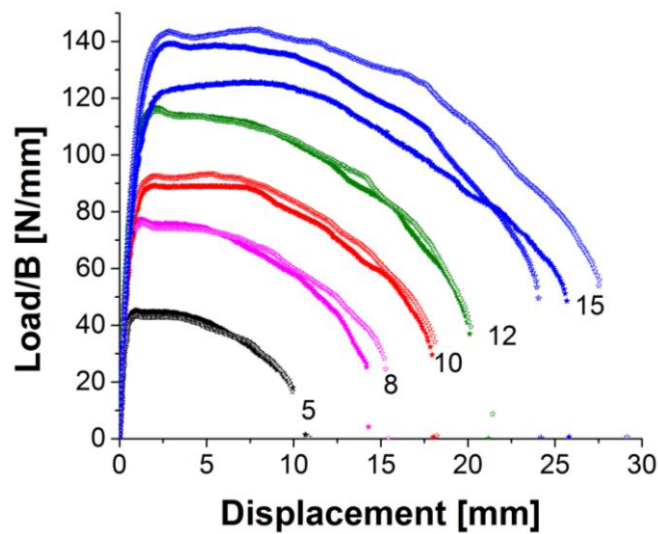

Figure 4.32 Curve Load/B-Displacement on Ecoflex samples

From each test it is possible to obtain a load-displacement curve, in particular, the graphs in Figure 4.32 show the load normalized on the thickness of the sample B. The area under the curve load/B-displacement represents the work of fracture referred to the thickness (W_f/B). In order to calculate the total specific energy of fracture, the area is divided also by the ligament length, L.

$$w_f = \frac{W_f}{BL} \tag{4.6}$$

To apply the EWF method the curves should be homothetic and the ligament has to be completely yielded. The former condition is roughly valid, as can be observed in figure. The latter could be verified observing the recorded video (Figure 4.34).
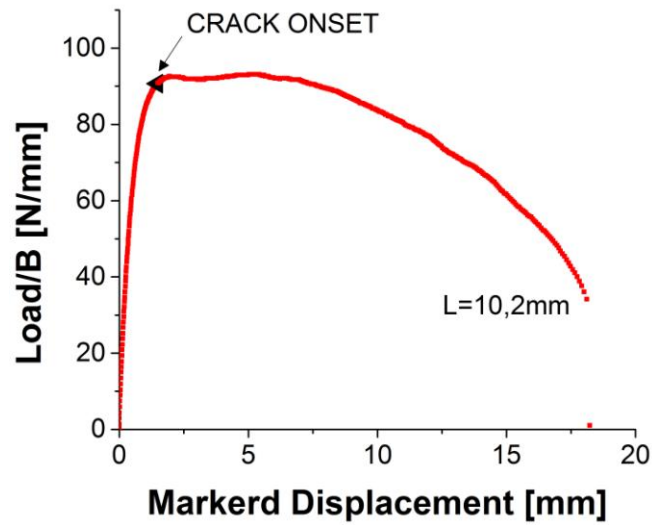
**Figure 4.33 Curve Load/B-Displacement on Ecoflex
sample at L=10,2 mm**
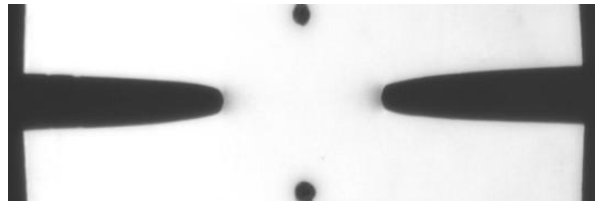
Figure 4.34 Crack onset of the previous curve

In the graph in Figure 4.33, one curve obtained from a fracture test, in particular on a sample with ligament length of 10,2 mm, is shown along with an image corresponding to the time at which fracture onset has been visually detected. The same point is indicated with a triangle on the Load/B-Displacement curve. It seems that in the case of Ecoflex the crack onset immediately before the whole ligament is yielding.

4.3.2. PBA-co-PBCHD100 70/30

For what concerns the copolymer 70/30, instead, the tests were performed only at 5, 10 and 15 mm ligament lengths, since the samples were 8 in all.
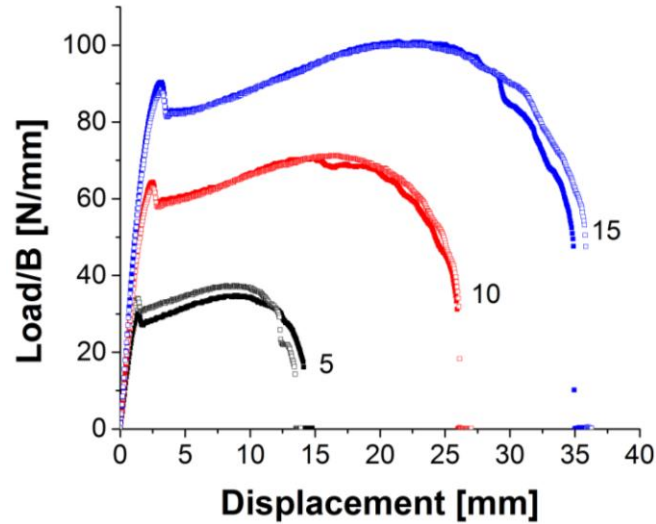
Figure 4.35 Curve Load/B-Displacement on copolymer 70/30 samples

In the Figure 4.35 the curves obtained from the different tests are shown, as it is possible to observe the curves seem to be homothetic. In this case, furthermore, on the contrary of the Ecoflex, the crack stars to propagate when the cross section is completely yielded, as it is shown in the graph in Figure 4.36 and in the correspondent frame (Figure 4.37).

**Figure 4.36 Curve Load/B-Displacement on copolymer
70/30 sample at L=10,085 mm**
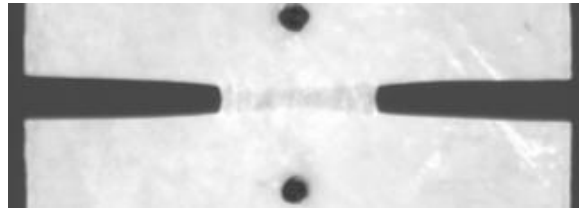
Figure 4.37 Crack onset of the previous curve

4.3.3.   Results analysis

From the previous curves where obtained different values of the work of fracture w_f, these data are reported in function of the ligament lengths and their validity was verified through a statistical method, which has confirmed the goodness of the linear regression both for the Ecoflex and the PBA-co-PBCHD100 70/30.
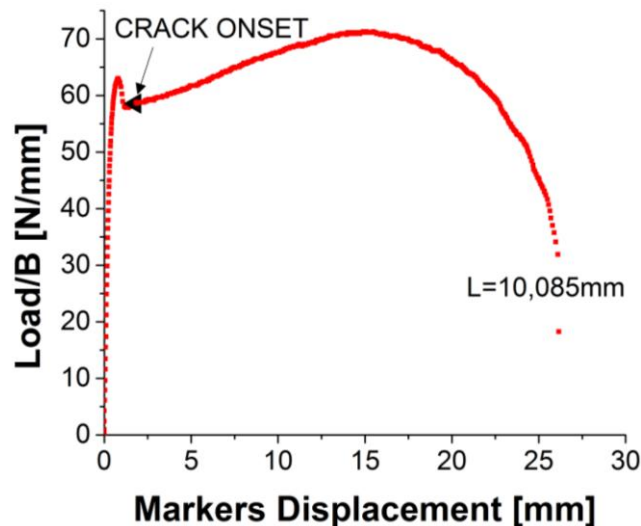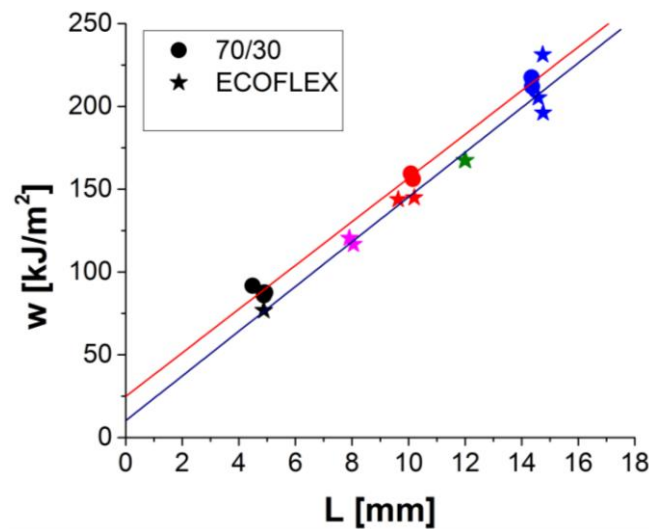

Figure 4.38 Work of fracture as function of ligament length both for Ecoflex and copolymer 70/30

Thence, from the fitting of the experimental data, it is possible to determine the essential work of fracture w_e of the two materials, as the intersection with the y-axis (L=0).

In graph xx both the fitting are shown and clearly appears that the Ecoflex value of the essential work of fracture is lower than the copolymer 70/30 w_e.

Table 4.8 Essential work of fracture of Ecoflex and copolymer 70/30

	ECOFLEX	PBA-co-PBCHD100 70/30.

w_e [kJ/m^2]	10.2± 8.6	24.7± 3.4

Recalling that the application field of this novel copolyester is the packaging, it is worth comparing it and the Ecoflex with a polymer widely used in the same file.

4.4. Comparison with other polymers used in packaging

Recalling that the application field of these novel copolyesters might be packaging, it is worth comparing them with Ecoflex and with a low-density polyethylene (LDPE) (32) (33), as it is widely used in the same field.

Starting from the characteristic temperatures (T_g and T_m) it is possible to observe that the glass transition temperatures of this new class of polymers are all higher than the LDPE but the same of the Ecoflex and, with the exception of PBCHD, at least 30°C below 0°C.

As for the melting temperatures instead, those of the PBA and copolymer 70/30 are significantly low, around 60°C and it may not be for packaging application or as mulch films for agriculture, another field in which Ecoflex and LDPE are applied. The copolymer 50/50 melting temperature, on the contrary, is higher, around 90°C, and about 10-20°C below the LDPE one.
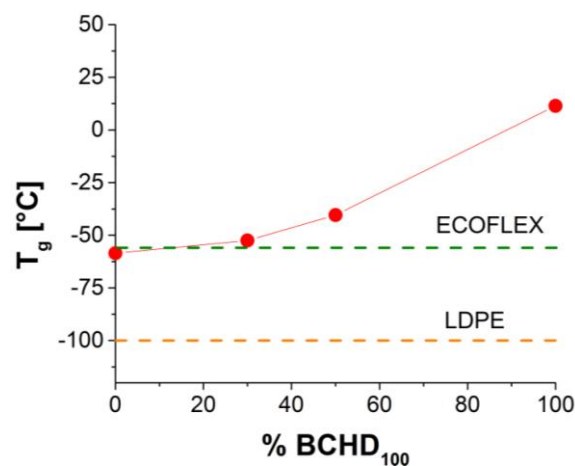

Figure 4.39 Comparison between the Tg in materials with Mw about 60000 and in LDPE and Ecoflex
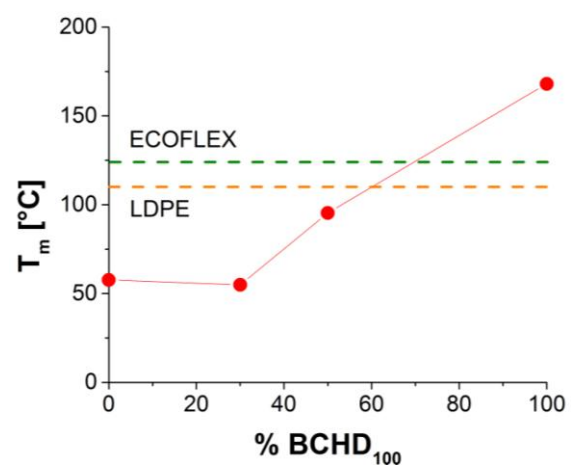
Figure 4.40 Comparison between the Tm in materials with Mw about 60000 and in LDPE and Ecoflex

Thus, from a thermal point of view, at room temperature these novel polyesters have an amorphous rubbery phase (quite far from glass transition) and a semicrystalline phase and are

expected to behave like the competitors. The only limitation for the copolymers with low BCHD content is low Tm which limit greatly their working temperature.
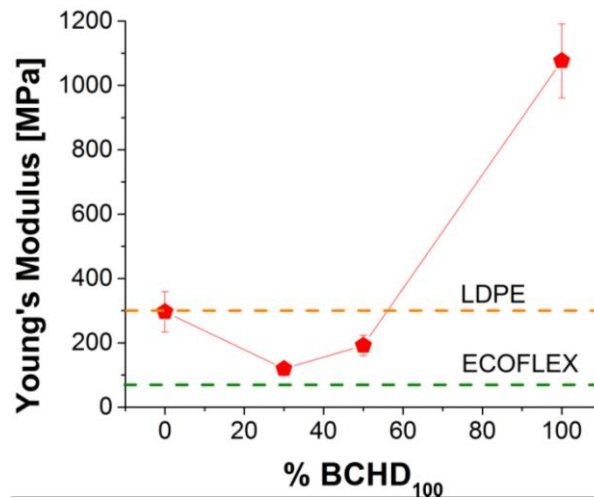

Figure 4.41 Mean Young's Modulus of the novel materials compared with those of the Ecoflex and of the LDPE

For what concerns the Young's Modulus, a first consideration on the comparison between the copolymers and the homopolymers, PBA and PBCHD, has to be carry out; indeed clearly appears that the values obtained for the former are lower than the PBA and PBCHD.

PBCHD is significantly stiffer, while PBA and copolymers display an intermediate behaviour between LDPE and Ecoflex, the most compliant of the considered materials. As for ultimate properties, Ecoflex is the most deformable of the considered materials, having the highest strains at yield and break, and shows a lower stress then LDPE. Both these materials show a peak in nominal stress-strain curves, followed by plastic flow and strain hardening. The same behaviour is typical of PBA and its copolymers - provided M_w is higher than about 50000 – but not for PBCHD. The values at yield and break are compared with those of the reference materials (Figure 4.42 - Figure 4.43 -Figure 4.44 - Figure 4.45). From this comparison, it can be concluded that, while PBCHD is significantly different than the referred materials and should maybe be considered for cases different than film for packaging or use in agriculture, PBA and PBA-co-PBCHD copolymers seem suitable to replace LDPE or Ecoflex. Among them it is important dwelling on the copolymer 50/50, since it sums up almost all the better properties of these materials, indeed it presents very good mechanical properties but also a relatively higher melting temperatures (90°C against the 58°C of the PBA).
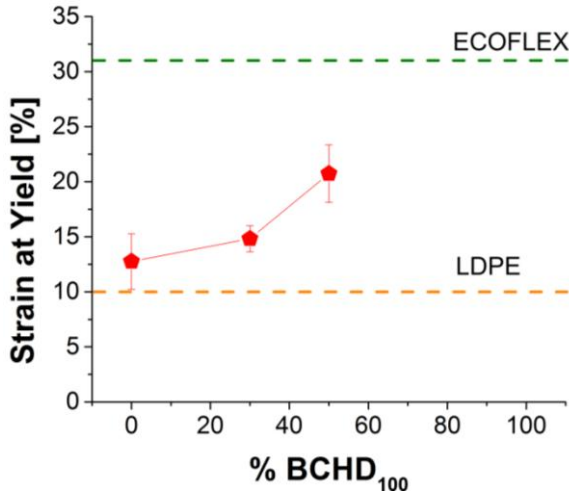
Figure 4.42 Comparison between the Strain at Yield in materials with Mw about 60000 and inLDPE and Ecoflex
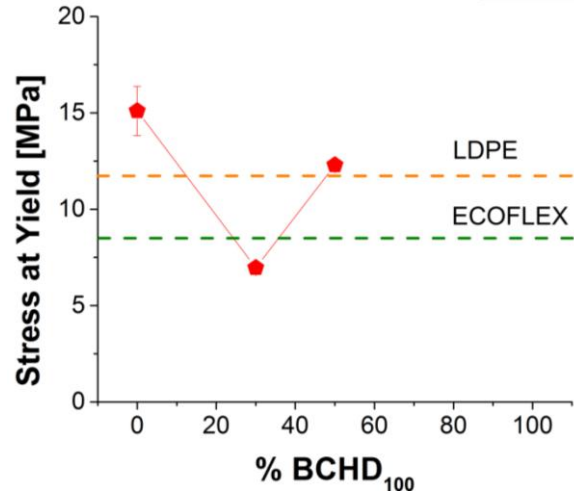
Figure 4.43 Comparison between the Stress at Yield in materials with Mw about 60000 and in LDPE and Ecoflex
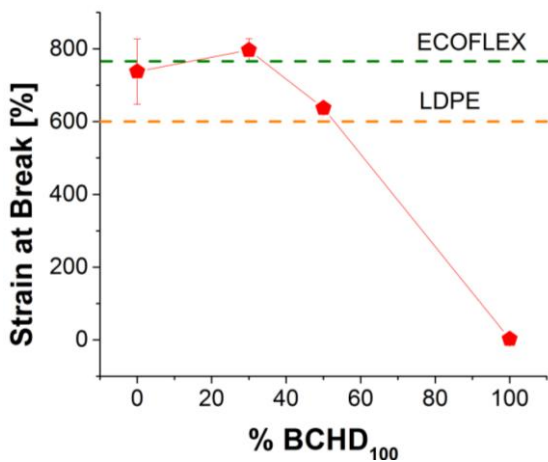
Figure 4.44 Comparison between the Strain at Break in materials with Mw about 60000 and in LDPE and Ecoflex

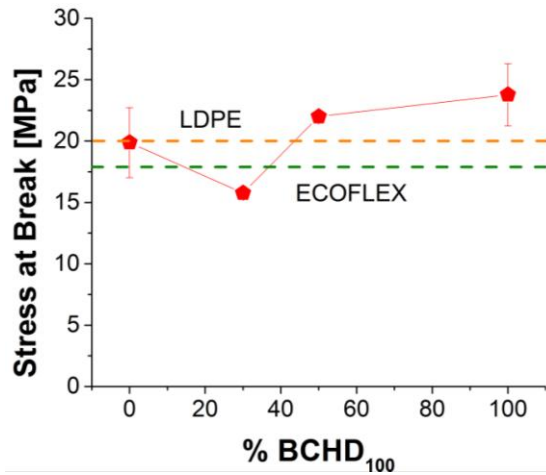**Figure 4.45 Comparison between the Stress at Break in materials with Mw about 60000 and in LDPE and Ecoflex**

Finally some considerations on the toughness of the material can be done comparing the experimental data obtained from the fracture tests, performed on the copolymer 70/30 and on the Ecoflex, with those given from literature for a low-density polyethylene (LDPE) (34) (35).
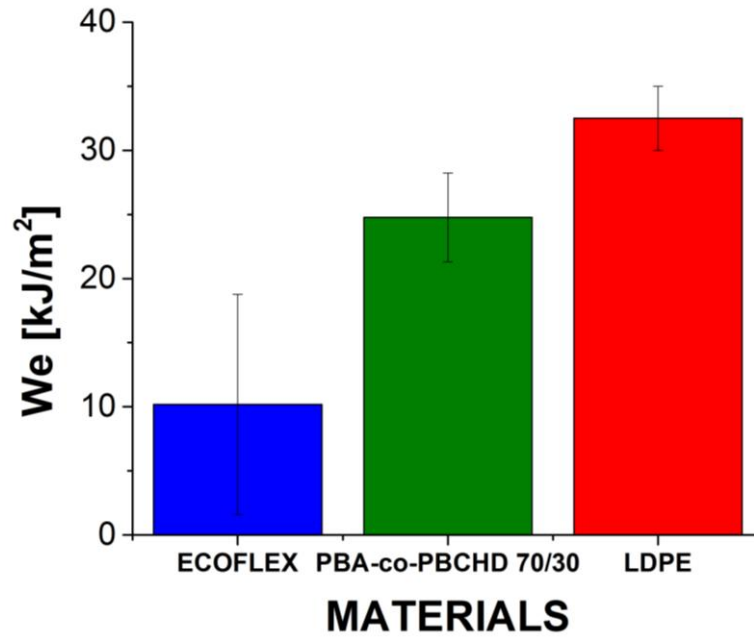
Figure 4.46 toughness of the novel materials compared with those of the Ecoflex and of the PE

As it is possible to observe the polyethylene shows a higher value for the essential work of fracture; nevertheless also the essential work of fracture obtained for the novel 70/30 copolymer is quite high and twice the Ecolex one.

If higher amount of material was available it would be interesting to carry out a deeper investigation on the essential work of fracture, in particular performing fracture tests on the copolymer 50/50, which is material that shows the most appropriate thermal and mechanical properties, in view of packaging application.

To this consideration, based on the mechanical and calorimetric investigation of this work, it has to be added that also processing of this materials seems relatively straightforward. As a matter of facts TGA characterization reported in (6) shows a high thermal resistance, and during sample preparation (by compression moulding) no significant degradation of the material was observed: even if in some cases the materials were processed twice before mechanical testing, no significant loss in response was observed. However, this topic would require deeper investigation.

Conclusive remarks

In this work some novel environmental-friendly copolyesters PBA-co-PBCHD$_{100}$ 70/30 and PBA-co-PBCHD$_{100}$ 50/50 were analysed from a calorimetric and mechanical point of view.

Considering the previous works, these materials were already characterized concerning their chemical structure, for example cis/trans ratio or their crystalline and amorphous phase, also as a function of the length of the aliphatic sequence. Moreover from a structural standpoint these copolyesters are similar to Ecoflex, a PBA-co-PBT, since the PBCHD and the PBT differ only on the presence of an aliphatic ring for the former and an aromatic one for the latter. The presence of the aliphatic ring, indeed, should increase the biodegradation rate, without reducing the mechanical and physical properties. In order to verify that the mechanical and physical properties of these copolyesters are appropriate for films used in packaging and agriculture, a comparison with LDPE, the widely used thermoplastic material in the field of packaging, and Ecoflex, an industrially available alternative to LDPE, were carried out.

From the literature works and the present calorimetric analysis, the homopolymers and the copolymers are semicrystalline. The thermal analysis, in accordance with the WAXD analysis, suggests that in the copolymer 50/50 the crystalline phase is constituted only by the BCHD$_{100}$ and in the same amount of the PBCHD$_{100}$. On the contrary in the case of the copolymer 70/30, the PBCHD content is very low and probably also the PBA takes part to the crystalline phase; this can explain why the copolymer 70/30 shows a low melting temperature, similar to the PBA one. In both the copolymer, instead, the amorphous phase is mainly given by the PBA.

According to the tensile tests all the novel materials show a transition from a relatively brittle to a ductile behaviour, when a threshold value of the molecular weight is crossed.

This estimated threshold value is around 60000 and above this value the stress and strain at break do not change significantly with M$_w$. On the contrary the Young's Modulus is not influenced by the molecular weight but on the BCHD content. Indeed the homopolymers show

higher values of Modulus, especially in the case of the PBCHD, which is a relatively brittle material. The Moduli of copolymers are lower and seem affected by the degree of crystallinity of the polymer.

Recalling the applications field of these novel copolyesters, they should be highly deformable and should show a good toughness. From a comparison with the LDPE, the widely used material in packaging field, and with the Ecoflex, the 70/30 and 50/50 copolyesters with high M_w (>60000), show a remarkable behaviour, for the elongation at break also better than the polyethylene one, while retaining comparable Moduli.

For what concerns the toughness of the materials, it was determined by EWF tests, only for the 70/30 copolymer and Ecoflex. The toughness of the 70/30 copolyester results lower than LDPE but considerably higher than Ecoflex.
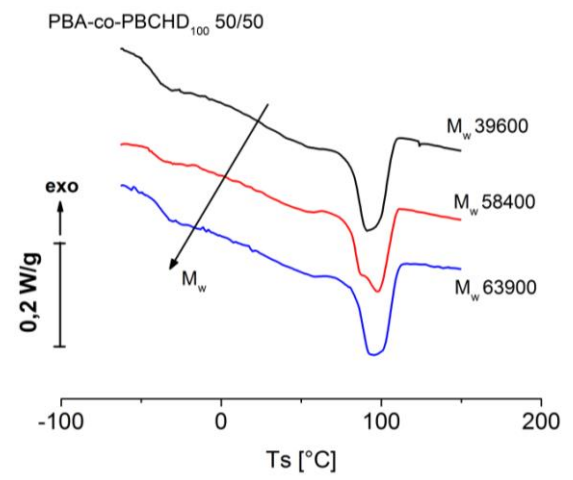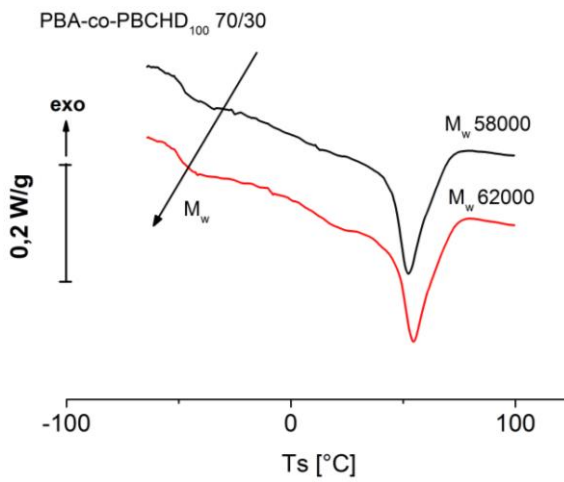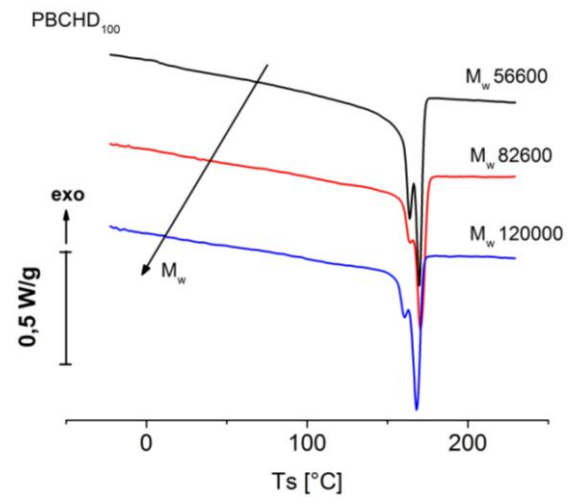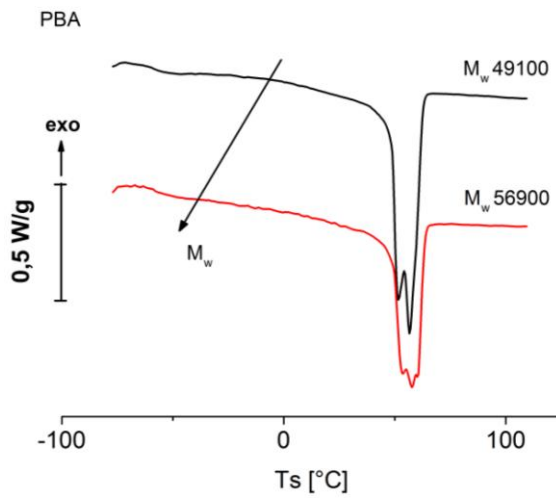
The results show the high potential of these studied novel copolymers as a future replacement of materials already in use.

Appendix

DSC cooling scans
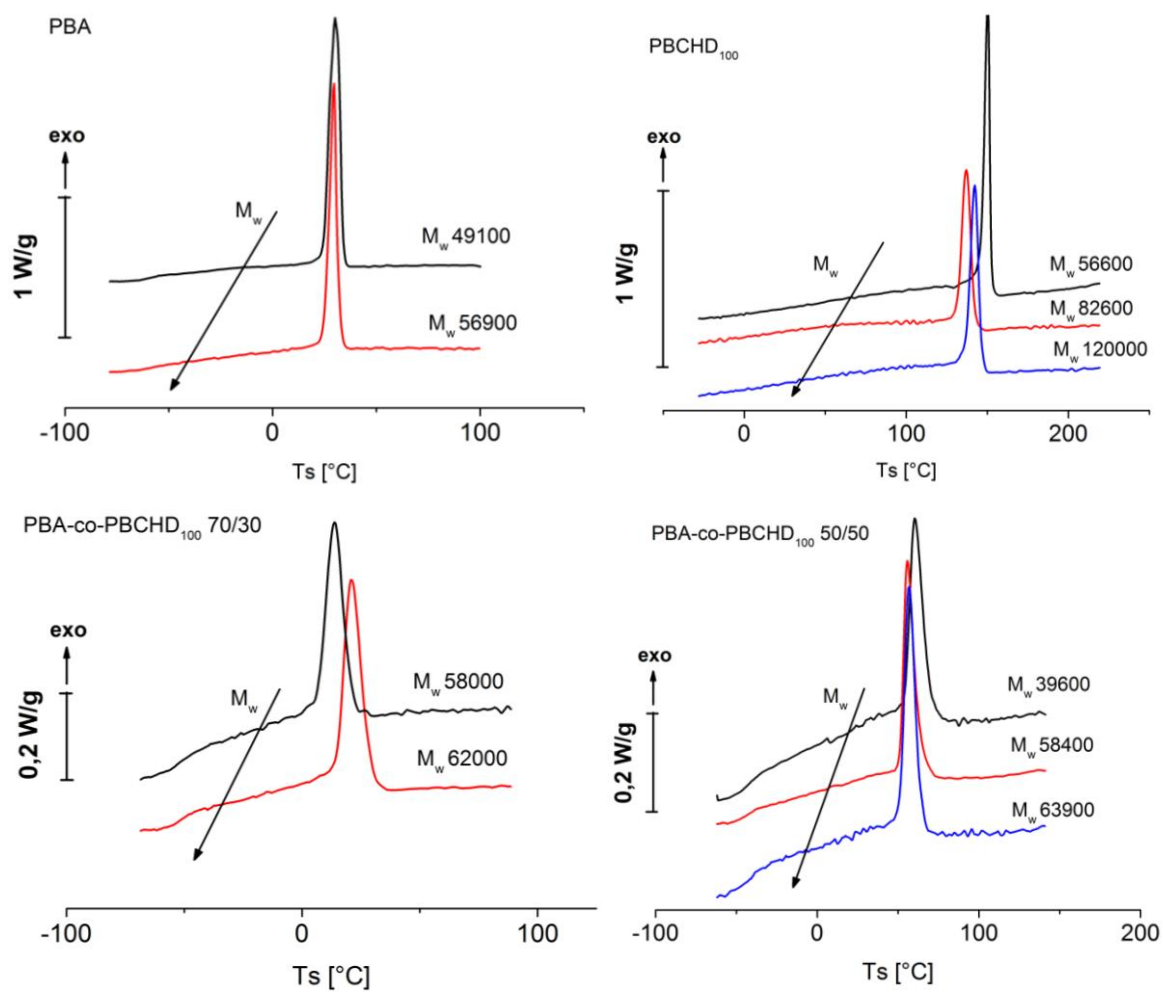
DSC II heating scans

Bibliography

1. **BASF.** *Ecoflex, Ecovio - Biodegradable polymers - inspired by nature* . 2008.

2. *Biodegradable mulch films for strawberry production.* **Bilck, Ana Paula ; Grossmann, Maria V.E. ; Yamashita Fabio.** 4, 2010, Polymer Testing, Vol. 29, p. 471-476.

3. *Influence of Molecular Structure and Stereochemistry of the 1,4- Cyclohexylene Ring on Thermal and Mechanical Behavior of Poly(butylene 1,4- cyclohexanedicarboxylate.* **Berti, Corrado, et al., et al.** 13, 2008, Macromolecular Chemistry and Physics, Vol. 209, p. 1333-1344.

4. *Novel copolyesters based on poly(alkylene dicarboxylate)s: 1. Thermal behavior and biodegradation of aliphatic–aromatic random copolymers.* **Berti, Corrado, et al., et al.** 11, 2008, European Polymer Journal, Vol. 44, p. 3650-3661.

5. *Novel copolyesters based on poly(alkylene dicarboxylate)s: 2. Thermal behavior and biodegradation of fully aliphatic random copolymers containing 1,4-cyclohexylene rings.* **Berti, Corrado, et al., et al.** 8, 2009, European Polymer Journal, Vol. 45, p. 2402-2412.

6. *Environmentally Friendly Copolyesters Containing 1,4-Cyclohexane Dicarboxylate Units, 1-Ralationships Between Chemical Structure and Thermal Properties.* **Berti, Corrado, et al., et al.** 2010, Macromolecular Journals, p. 1559–1571.

7. **Sullalti, Simone.** *New Eeco-friendly Polyesters from Renewable Resources.* Alma Master Studiotum - Università di Bologna. 2012. Ph.D. dissertation.

8. *The effect of aliphatic chain length on thermal properties of poly(alkylene dicarboxylate)s.* **Berti C., Celli A., Marchese P. Marianucci E. Barbiroli G. Di Credico F.** 2007, EPOLYMERS,, Vol. 057, p. 1 – 18.

9. *Thermal properties of poly(alkylene dicarboxylate)s derived from 1,12-dodecanedioic acid and even aliphatic diols.* **Celli A., Barbiroli G., Berti C. Di Credico F. Lorenzetti C.**

Marchese P. Marianucci E. 2007, Journal of Polymer Science, Part B: Polymer Physics, Vol. 45, p. 1053-1067.

10. *Eco-friendly Poly(butylene 1,4-cyclohexanedicarboxylate): Relationships Between Stereochemistry and Crystallization Behavior.* **Celli, A ; Marchese, P ; Sullalti S ; Berti C ; Barbiroli G.** 14, 2011, Macromolecular Chemistry And Physics, Vol. 212, p. 1524-1534.

11. *Aliphatic/aromatic copolyesters containing biobased ?-hydroxyfatty acids: Synthesis and structure–property relationships.* **Celli, Annamaria ; Marchese, Paola ; Sullalti Simone ; Cai Jiali ; Gross Richard A.** 15, 2013, Polymer, Vol. 54, p. 3774-3783.

12. *About durability of biodegradable polymers: structure/degradability relationship.* **Commereuc S., Askanian H., Verney V. Celli A. Marchese P.** 2010, Macromol. Symp., Vol. 296, p. 378-387.

13. **T.L.Anderson.** *Fracture Mechanics: fundamentals and applications, 2nd Edition.* s.l. : CRC Press, 1995.

14. *On stable crack growth.* **Broberg, K.B.** 1975, Journal of the Mechanics and Physics of Solids, Vol. 3, p. 215-237.

15. *The essential work of plane stress ductile fracture.* **B.Cotterell, J.K. Reddel.** 1977, International Journal of fracture, Vol. 13, p. 267-277.

16. *The essential work of fracture for tearining ductile metals.* **Y.W.Mai, B.Cotterell.** 1984, International Journal of fracture, Vol. 24, p. 229-236.

17. *On the essential work of ductile fracture in polymers.* **Y.W.Mai, B.Cotterell.** 1986, International Journal of fracture, Vol. 32, p. 105-125.

18. *The essential fracture work concept for toughness measurement of ductile polymers.* **J.Wu, Y.W.Mai.** 1996, Polymer engineering and science, Vol. 36, p. 2275-2288.

19. *ESIS Test Protocol: essential work of fracture and cohesive zone fracture toughness.* **E.Clutton.** 2002, ESIS Publication.

20. **A.Celli, Prof.** *Private communication.* s.l. : Università di Bologna, 11/01/2013.

21. *Application of the essential work of fracture (EWF) concept for polymers, related blends and composites: a review.* **T.Báráni, T.Czigány, J.Karger-Kocsis.** 2010, Progress in Polymer Science, Vol. 35, p. 1257-1287.

22. **Fazzini, Sara.** *Caratterizzazione del comportamento a frattura di materiali polimerici in stato di sforzo piano: confronto tra lavoro essenziale di frattura e integrale J.* Politecnico di Milano. 2010-2011. Master's thesis.

23. **F.Meneghello.** *Il lavoro essenziale di frattura come misura della tenacitò di film polimerici: influenza della viscoelasticità.* Politecnico di Milano – Dipartimento di Chimica, Materiali e Ingegneria Chimica "Giulio Natta". 2006-2007. Master's thesis.

24. *Use of extensometers on essential work of fracture (EWF) tests.* **J. Gamez-Perez, O. Santana, A.B. Martinez M.Ll. Maspoch.** 2008, Polymer Testing, Vol. 27, p. 491-497.

25. *The standardization of the EWF test.* **J.G. Williams, M.Rink.** 2007, Engineering Fracture Mechanics, Vol. 74, p. 1009-1017.

26. **B.Wunderlich.** *Macromolecular Physics. 3: Crystal Melting.* New York : Academic press, 1980.

27. The Advanced Thermal Analysis System . *http:/athas.prz.rzeszow.pl/.* [Online]

28. *A Model Treating Tensile Deformation of Semicrystalline Polymers: Quasi-Static Stress−Strain Relationship and Viscous Stress Determined for a Sample of Polyethylene.* **Hong, K., Rastogi, A. e Strobl, G.** . : Macromolecules, 2004, Vol. 37(26). 10165-10173.

29. *Critical strains determining the yield behaviour of s-PP*.* **Men, Y. e Strobl, G.** s.l. : Journal of Macromolecular Science, Part B, 2001, Vol. 40(5). 775-796.

30. *Elasticity of syndiotactic polypropylene: Insights from temperature and time dependence.* **Guadagno, Liberata, Naddeo, Carlo e Vittoria, Vittoria.** s.l. : European Polymer Journal, 2009, Vol. 45(8). 2192-2201.

31. **Perillo, Nadia.** *Stereoregularity degree effect on the deformation mechanisms in syndiotactic polypropylenes and comparison with isotactic polypropylene.* s.l. : Politecnico di Milano, 2012.

32. *Network stretching, slip processes, and fragmentation of crystallites during uniaxial drawing of polyethylene and related copolymers. A comparative study.* **Hiss, R ; Hobeika, S ; Lynn C ; Strobl G.** 13, 1999, Macromolecules, Vol. 32, p. 4390-4403.

33. CES EduPack 2013. *http://ces-edupack-2013.software.informer.com/.* [Online]

34. *On the essential work of fracture of linear low-density-polyethylene. I. Precision of the testing method.* **Pegoretti, A., et al., et al.** s.l. : Engineering Fracture Mechanics, 2009, Vol. 76(18). 2788-2798 .

35. *Evaluation of the tear properties of polyethylene blown films using the essential work of fracture concept.* **Choi, Byoung-Ho, et al., et al.** s.l. : Polymer, 2010, Vol. 51(21). 2732-2739.